Brain Struct Funct (2016) 221:1033–1065
DOI 10.1007/s00429-014-0954-y

ORIGINAL ARTICLE

Afferent projections to the different medial amygdala subdivisions: a retrograde tracing study in the mouse

Bernardita Cádiz-Moretti · Marcos Otero-García · Fernando Martínez-García · Enrique Lanuza

Received: 20 June 2014 / Accepted: 30 November 2014 / Published online: 11 December 2014

Abstract The medial amygdaloid nucleus (Me) is a key node in the socio-sexual brain, composed of anterior (MeA), posteroventral (MePV) and posterodorsal (MePD) subdivisions. These subdivisions have been suggested to play a different role in reproductive and defensive behaviours. In the present work we analyse the afferents of the three Me subdivisions using restricted injections of fluorogold in female outbred CD1 mice. The results reveal that the MeA, MePV and MePD share a common pattern of afferents, with some differences in the density of retrograde labelling in several nuclei. Common afferents to Me subdivisions include: the accessory olfactory bulbs, piriform cortex and endopiriform nucleus, chemosensory amygdala (receiving direct inputs from the olfactory bulbs), posterior part of the medial bed nucleus of the stria terminalis (BSTM), CA1 in the ventral hippocampus and posterior intralaminar thalamus. Minor projections originate from the basolateral amygdala and amygdalo-hippocampal area, septum, ventral striatum, several allocortical and periallocortical areas, claustrum, several hypothalamic structures, raphe and parabrachial complex. MeA and MePV share minor inputs from the frontal cortex (medial orbital, prelimbic, infralimbic and dorsal peduncular cortices), but differ in the lack of main olfactory projections to the MePV. By contrast, the MePD receives preferential projections from the rostral accessory olfactory bulb, the posteromedial BSTM and the ventral premammillary nucleus. In summary, the common pattern of afferents to the Me subdivisions and their interconnections suggest that they play cooperative instead of differential roles in the various behaviours (e.g., sociosexual, defensive) in which the Me has been shown to be involved.

Keywords Vomeronasal · Olfactory system · Fluorogold · Retrograde tracing · Socio-sexual behaviour

Abbreviations

1	Layer 1
2	Layer 2
2Cb	2nd cerebellar lobule
3	Layer 3
3V	3rd ventricle
4V	4th ventricle
7n	Facial nerve or its root
8n	Vestibulocochlear nerve
8vn	Vestibular root of the vestibulocochlear nerve
AA	Anterior amygdaloid area
AAD	Anterior amygdaloid area, dorsal part
AAV	Anterior amygdaloid area, ventral part
aca	Anterior commissure, anterior part
aci	Anterior commissure, intrabulbar part
Acb	Accumbens nucleus
AcbC	Accumbens nucleus, core
AcbSh	Accumbens nucleus, shell
ACo	Anterior cortical amygdaloid nucleus
AH	Anterior hypothalamic area
AHA	Anterior hypothalamic area, anterior part
AHC	Anterior hypothalamic area, central part

B. Cádiz-Moretti · M. Otero-García · F. Martínez-García · E. Lanuza (✉)
Laboratori de Neuroanatomia Funcional Comparada, Departaments de Biologia Cel·lular and Biologia Funcional, Facultat de Ciències Biològiques, Universitat de València, C/Dr. Moliner, 50, Burjassot, 46100 Valencia, Spain
e-mail: Enrique.Lanuza@uv.es

Present Address:
F. Martínez-García
Unitat Predepartamental de Medicina, Fac. Ciències de la Salut, Universitat Jaume I, Av. Sos Baynat, s/n; Campus del Riu Sec, 12071 Castellón de la Plana, Spain

AHi	Amygdalohippocampal area
AHP	Anterior hypothalamic area, posterior part
AI	Agranular insular cortex
AID	Agranular insular cortex, dorsal part
AIP	Agranular insular cortex, posterior part
AIV	Agranular insular cortex, ventral part
AOB	Accessory olfactory bulb
AOM	Anterior olfactory nucleus, medial part
AON	Anterior olfactory nucleus
AOP	Anterior olfactory nucleus, posterior part
APir	Amygdalopiriform transition area
Aq	Aqueduct
Arc	Arcuate hypothalamic nucleus
BAOT	Bed nucleus of the accessory olfactory tract
BLA	Basolateral amygdaloid nucleus, anterior part
BLP	Basolateral amygdaloid nucleus, posterior part
BLV	Basolateral amygdaloid nucleus, ventral part
BMA	Basomedial amygdaloid nucleus, anterior part
BMP	Basomedial amygdaloid nucleus, posterior part
BST	Bed nucleus of the stria terminalis
BSTIA	BST, intraamygdaloid division
BSTLP	BST, lateral division, posterior part
BSTLV	BST, lateral division, ventral part
BSTMA	BST, medial division, anterior part
BSTMPI	BST, medial division, posterointermediate part
BSTMPL	BST, medial division, posterolateral part
BSTMPM	BST, medial division, posteromedial part
BSTMV	BST, medial division, ventral part
BSTS	Bed nucleus of stria terminalis, supracapsular part
CA1	Field CA1 of hippocampus
CA3	Field CA3 of hippocampus
Ce	Central amygdaloid nucleus
CeC	Central amygdaloid nucleus, capsular part
CeL	Central amygdaloid nucleus, lateral division
CeM	Central amygdaloid nucleus, medial division
Cl	Claustrum
CM	Central medial thalamic nucleus
cp	Cerebral peduncle
CPu	Caudate putamen
csc	Commissure of the superior colliculus
cst	Commissural stria terminalis
CxA	Cortex-amygdala transition zone
D3V	Dorsal 3rd ventricle
DEn	Dorsal endopiriform nucleus
DG	Dentate gyrus
dlot	Dorsal lateral olfactory tract
DM	Dorsomedial hypothalamic nucleus
DP	Dorsal peduncular cortex
DR	Dorsal raphe nucleus
DTT	Dorsal tenia tecta
E/OV	Ependymal and subependymal layer/olfactory ventricle
ec	External capsule
EPl	External plexiform layer of the main olfactory bulb
EPlA	External plexiform layer of the accessory olfactory bulb
f	Fornix
fi	Fimbria of the hippocampus
fmi	Forceps minor of the corpus callosum
fr	Fasciculus retroflexus
Gl	Glomerular layer of the main olfactory bulb
GlA	Glomerular layer of the AOB
GrA	Granule cell layer of the AOB
GrO	Granular cell layer of the main olfactory bulb
HDB	Nucleus of the horizontal limb of the diagonal band
I	Intercalated nuclei of the amygdala
ic	Internal capsule
IL	Infralimbic cortex
IM	Intercalated amygdaloid nucleus, main part
IP	Interpeduncular nucleus
IPAC	Interstitial nucleus of the posterior limb of the anterior commissure
IPl	Internal plexiform layer of the main olfactory bulb
LA	Lateroanterior hypothalamic nucleus
La	Lateral amygdaloid nucleus
LaDL	Lateral amygdaloid nucleus, dorsolateral part
LaVL	Lateral amygdaloid nucleus, ventrolateral part
LaVM	Lateral amygdaloid nucleus, ventromedial part
LC	Locus coeruleus
Ld	Lambdoid septal zone
LDTg	Laterodorsal tegmental nucleus
LEnt	Lateral entorhinal cortex
LGP	Lateral globus pallidus
LH	Lateral hypothalamic area
LHb	Lateral habenular nucleus
LPB	Lateral parabrachial nucleus
LPO	Lateral preoptic area
LO	Lateral orbital cortex
lo	Lateral olfactory tract
LOT	Nucleus of the lateral olfactory tract
LPO	Lateral preoptic area
LSD	Lateral septal nucleus, dorsal part
LSI	Lateral septal nucleus, intermediate part
LSV	Lateral septal nucleus, ventral part
LV	Lateral ventricle
mcp	Middle cerebellar peduncle
MCPO	Magnocellular preoptic nucleus
MD	Mediodorsal thalamic nucleus
ME	Median eminence

Me	Medial amygdaloid nucleus
me5	Mesencephalic trigeminal tract
MeA	Medial amygdaloid nucleus, anterior subnucleus
MeAD	Medial amygdaloid nucleus, anterodorsal part
MeAV	Medial amygdaloid nucleus, anteroventral part
MePD	Medial amygdaloid nucleus, posterodorsal subnucleus
MePV	Medial amygdaloid nucleus, posteroventral subnucleus
MGD	Medial geniculate nucleus, dorsal part
MGM	Medial geniculate nucleus, medial part
MGV	Medial geniculate nucleus, ventral part
MHb	Medial habenular nucleus
Mi	Mitral cell layer of the main olfactory bulb
MiA	Mitral cell layer of the AOB
ml	Medial lemniscus
mlf	Medial longitudinal fasciculus
MM	Medial mammillary nucleus, medial part
MnR	Median raphe nucleus
MO	Medial orbital cortex
Mo5	Motor trigeminal nucleus
MOB	Main olfactory bulb
MPA	Medial preoptic area
MPB	Medial parabrachial nucleus
MPO	Medial preoptic nucleus
MS	Medial septal nucleus
mt	Mammillothalamic tract
mtg	Mammillotegmental tract
ns	Nigrostriatal bundle
opt	Optic tract
ox	Optic chiasm
Pa	Paraventricular hypothalamic nucleus
PAG	Periaqueductal gray
PB	Parabrachial nucleus
pc	Posterior commissure
Pe	Periventricular hypothalamic nucleus
PH	Posterior hypothalamic area
PIL	Posterior intralaminar thalamic nucleus
Pir	Piriform cortex
PLCo	Posterolateral cortical amygdaloid nucleus
PMCo	Posteromedial cortical amygdaloid nucleus
PMD	Premammillary nucleus, dorsal part
PMV	Premammillary nucleus, ventral part
PnC	Pontine reticular nucleus, caudal part
Po	Posterior thalamic nuclear group
PP	Peripeduncular nucleus
Pr5VL	Principal sensory trigeminal nucleus, ventrolateral part
PRh	Perirhinal cortex
PrL	Prelimbic cortex
pv	Periventricular fibre system
PV	Paraventricular thalamic nucleus
PVA	Paraventricular thalamic nucleus, anterior part
PVP	Paraventricular thalamic nucleus, posterior part
py	Pyramidal tract
Re	Reuniens thalamic nucleus
RLi	Rostral linear nucleus of the raphe
S	Subiculum
s5	Sensory root of the trigeminal nerve
scp	Superior cerebellar peduncle
SG	Supragenicular thalamic nucleus
SHi	Septohippocampal nucleus
SI	Substantia innominata
SL	Semilunar nucleus
sm	Stria medullaris
SNR	Substantia nigra, reticular part
sox	Supraoptic decussation
sp5	Spinal trigeminal tract
SPF	Subparafascicular thalamic nucleus
SPFPC	Subparafascicular thalamic nucleus, parvicellular part
st	Stria terminalis
str	Superior thalamic radiation
Su5	Supratrigeminal nucleus
SuM	Supramammillary nucleus
TC	Tuber cinereum area
Tu	Olfactory tubercle
VDB	Nucleus of the vertical limb of the diagonal band
VEn	Ventral endopiriform nucleus
VL	Ventrolateral thalamic nucleus
VMH	Ventromedial hypothalamic nucleus
VO	Ventral orbital cortex
VP	Ventral pallidum
vsc	Ventral spinocerebellar tract
VTA	Ventral tegmental area
VTT	Ventral tenia tecta
ZI	Zona incerta
ZID	Zona incerta, dorsal part
ZIV	Zona incerta, ventral part

Introduction

The medial amygdaloid nucleus of the amygdala (Me) is one of the main structures receiving the projections originated in the accessory olfactory bulb (Scalia and Winans 1975). As a consequence, it is considered part of the so-called chemosensory amygdala, together with other nuclei receiving direct inputs from the main and/or accessory olfactory bulbs, e.g. the cortical nuclei of the amygdala, the nuclei of the lateral and accessory olfactory tracts and a part of the medial posterior bed nucleus of the stria

terminalis (Table 1; Gutiérrez-Castellanos et al. 2010). In addition, the Me was very early identified as a relevant structure for the control of sexual behaviour in male hamsters (Lehman et al. 1980). Consequently, the Me has been proposed to be a key node of the sexually dimorphic network mediating socio-sexual behaviours in rodents (Newman 1999) and other vertebrates (Goodson 2005), which is typically enriched in neurones expressing steroid hormone receptors (Simerly et al. 1990). In fact, there is solid evidence indicating that the Me is involved in the control of aggression (Koolhaas et al. 1990; Sano et al. 2013; Wang et al. 2013), parental care (Morgan et al. 1999; Oxley and Fleming 2000; Tachikawa et al. 2013), intersexual recognition (Moncho-Bogani et al. 2005; Bergan et al. 2014) and mating (Hari dass and Vyas 2014), as well as in other behaviours and physiological processes.

Thus, understanding the neuroanatomical substrate of social behaviours requires a close analysis of the connections of the Me. The efferent projections of the Me have been previously characterized in several rodent species including hamsters (Gomez and Newman 1992; Coolen and Wood 1998; Maras and Petrulis 2010a), rats (Canteras et al. 1995) and mice (Usunoff et al. 2009; Pardo-Bellver et al. 2012). The results of those studies indicate that the anterior (MeA), posteroventral (MePV) and posterodorsal (MePD) subdivisions of the Me show some differential projections. These anatomical data suggest that the posterodorsal part is mainly involved in reproductive behaviours, whereas the posteroventral part plays a role in the expression of defensive reactions, in particular elicited by predator-derived chemicals (Choi et al. 2005).

However, recent findings about the type of information perceived by the vomeronasal organ (VNO) have revealed that, in addition to reproductive-related signals and predator-derived cues (Papes et al. 2010; Isogai et al. 2011), the VNO detects chemical signals from competitors (Chamero et al. 2007), stress-related signals (Nodari et al. 2008) and illness cues (Riviere et al. 2009). Therefore, the view of the medial amygdala as a relevant nucleus processing sexually relevant signals versus chemicals from predators should be revised taking into account these other possible types of information. Moreover, the Me also receives direct projections from the main olfactory bulb (Scalia and Winans 1975; Pro-Sistiaga et al. 2007; Kang et al. 2009, 2011; Cadiz-Moretti et al. 2013), and therefore it is also a critical node to integrate olfactory and vomeronasal information.

To fully understand how the Me processes the information derived from the different types of olfactory- and vomeronasal-detected chemicals, it is necessary to identify the rest of the neural inputs received by this nucleus, and in particular by its subdivisions. However, the topography of the afferents to the subnuclei of the Me has not been studied in detail in any mammalian species. In fact, our knowledge about the inputs to the Me derive from a number of anterograde tracing studies of some of the structures giving rise to projections to the Me (see, for a review, Pitkanen 2000), and a few studies using retrograde tracers encompassing several of the Me subdivisions (Coolen and Wood 1998; Ottersen and Ben-Ari 1979; Veening 1978). Anatomical information is available mainly for rats (and, to a lesser extent, for hamsters). By contrast, very little information is available for mice, a species used in a large number of behavioural experiments to understand the role of the vomeronasal system (Halpern and Martinez-Marcos 2003). These studies have benefited from the availability of genetically modified mice with alterations of key genes for the function of the vomeronasal organ, which have yielded relevant new information on the neural basis of socio-sexual behaviours (Tirindelli et al. 2009; Zufall and Leinders-Zufall 2007).

Table 1 The amygdaloid structures receiving direct projections from the olfactory bulbs are considered as the chemosensory amygdala

Chemosensory amygdaloid subdivision	Amygdaloid structures
Olfactory amygdala	Posterolateral cortical amygdaloid nucleus
	Amygdalo-piriform transition area
Vomeronasal amygdala	Posteromedial cortical amygdaloid nucleus
	Posterior part of the posterior division of the bed nucleus of the stria terminalis
Mixed chemosensory amygdala	
Olfactory predominance	Anterior cortical amygdaloid nucleus
	Cortex-amygdala transition zone
	Nucleus of the lateral olfactory tract
Vomeronasal predominance	Medial amygdaloid nucleus
	Bed nucleus of the accessory olfactory tract
	Anterior amygdaloid area

Structures receiving inputs only from the main olfactory bulb constitute the olfactory amygdala. Those receiving inputs only from the accessory olfactory bulb form the vomeronasal amygdala. Finally, those receiving inputs from both the main and accessory olfactory bulbs are considered the mixed chemosensory amygdala

With the aim to comprehensively describe the neuroanatomical inputs to the different subdivisions of the medial amygdala, in the present study, we have traced the afferent projections to the anterior, posterodorsal and posteroventral subdivisions of the Me by using the retrograde tracer fluorogold.

Materials and methods

Animals

For the present study, we used 21 adult female mice (*Mus musculus*) from the CD1 strain (Janvier, Le Genest Saint-

Isle, France), which were 8–27 weeks old and weighed 26.5–53.2 g. CD1 (also called ICR) is an outbred mouse strain with a good reproductive rate, docile and useful for analysis of social and sexual behaviours. In our laboratory we have extensively used it in the analysis of the attractive properties of male chemosignals in female mice (e.g. Moncho-Bogani et al. 2005) and its neurobiological substrate (e.g. Martinez-Ricos et al. 2008; Agustin-Pavón et al. 2014) including tract-tracing studies of the relevant connections (Pardo-Bellver et al. 2012; Cadiz-Moretti et al. 2013).

Mice were kept in cages with food and water ad libitum in a 12 h light: dark cycle at 25–26 °C. We treated the mice according to the guidelines of the European Union Council Directive of June 3rd, 2010 (6106/1/10 REV1). The Committee of Ethics on Animal Experimentation of the University of Valencia approved the experimental procedures.

Surgery and tracer injections

For surgery, animals received isofluorane (2–2.5 %) delivered in oxygen (1–1.3 L/min) (MSS Isoflurane Vaporizer, Medical Supplies and Services, UK) as anaesthetic using a mouse anaesthetic mask. They also received a subcutaneous butorfanol injection (5 mg/kg, Turbugesic, Pfizer, New York, USA) as analgesic. After fixing the mouse head in the stereotaxic apparatus (David Kopf, 963-A, Tujunga CA, USA), we drilled a small hole above the target zone.

To study the afferents to the three subdivisions of the medial amygdaloid nucleus, mice received iontophoretic injections of the fluorescent retrograde tracer Fluoro-Gold (FG) (Hydroxystilbamidine bis(methanesulfonate), Sigma-Aldrich, Cat # 39286) diluted at 2 % in distilled water. We delivered the tracer from a glass micropipette (20–30 μm diameter tips) by means of positive current pulses (7on/7off, 3 μA) during 3 min. To avoid diffusion of the tracer along the pipette track, we applied a mild retention current (−0.1 μA) during the entrance and withdrawal of the micropipette and left it in place for 10 min after finishing the injection. Injection coordinates relative to Bregma were adapted to the CD1 mice from the atlas of the mouse brain (Paxinos and Franklin 2001) as follows: MeA: AP −1.40 to −1.45 mm, L −2.0 to −2.1 mm, DV −5.55 to −5.60 mm; MePV: AP −1.9 mm, L −2.05 to −2.10 mm, DV −5.48; MePD: AP −1.9 mm, L −2.1 mm and DV −5.18 mm.

After the injection, we closed the wound with Histoacryl (Braun, Tuttlinger, Germany). During the whole procedure, animals rested on a thermic blanket to maintain their body temperature, and they received eye drops (Siccafluid, Thea S.A Laboratories, Spain) to prevent eye ulceration.

Histology

After 6–8 days of survival, we deeply anaesthetized the animals with an overdose of sodium pentobarbital (intraperitoneal, 100 mg/kg, Eutanax, Laboratorios Normon S.A. Madrid, Spain) and perfused them transcardially with saline solution (0.9 %) followed by 4 % paraformaldehyde diluted in phosphate buffer (PB; 0.1 M, pH 7.6). Following perfusion, brains were removed from the skulls, postfixed for 4 h in the same fixative and cryoprotected in 30 % sucrose in PB (0.1 M, pH 7.6) at 4 °C until they sank. We used a freezing microtome to obtain sagittal sections (30 μm) from the bulbs and frontal sections (40 μm) from the rest of the brain. In both cases, sections were collected in four parallel series.

After checking the location of the FG injection using fluorescence microscopy, we processed the sections of one of the series of each brain for free-floating immunoperoxidase detection of FG. To do so, we first inactivated endogenous peroxidase activity with 1 % H_2O_2 in Tris-buffered saline (TBS) (0.05 M, pH 7.6) for 15 min. Then, we incubated the sections in a blocking solution of TBS with 0.3 % Triton X-100 (TBS-Tx) containing 8 % of normal goat serum (NGS) and 4 % of bovine serum albumin (BSA), for 2 h at room temperature (RT). After that, we sequentially incubated the sections in: rabbit anti-Fluorescent Gold (Millipore, Cat # AB153) diluted 1:3,000 in TBS-Tx with 4 % NGS and 2 % BSA overnight at 4 °C; biotinyled goat anti-rabbit IgG (Vector, Cat # BA-1,000) diluted 1:200 in TBS-Tx with 4 % NGS for 2 h at room temperature; and ABC Elite (Vectastain ABC elite kit, Vector Labs, Burlingame, CA, USA) diluted 1:50 in TBS-Tx for 2 h at room temperature. Finally we revealed the resulting peroxidase labelling with 0.0025 % diaminobenzidine in PB (0.1 M, ph 8.0) with 0.01 % H_2O_2.

The anti-FG antibody has been previously validated in many papers (e.g. Gutiérrez-Castellanos et al. 2014; summarized in the *Journal of Comparative Neurology* antibody database, available at http://onlinelibrary.wiley.com/journal/10.1002/(ISSN)1096-9861/homepage/jcn_antibody_database.htm). We also checked that the omission of the primary antibody resulted in no labelling in our brain tissue.

Sections were mounted onto gelatinized slides, dehydrated in alcohols, cleared with xylene and covereslipped with Entellan (Merck Millipore, Cat # 1079610100). To facilitate the identification of the neural structures containing retrogradely labelled cells, in most cases we processed a second series of sections for FG immunohistochemistry and counterstained them with Nissl staining.

Image acquisition and processing

We observed the sections using an Olympus CX41RF-5 microscope and photographed them using a digital Olympus XC50 camera. Fluorescent images of the FG injection sites (shown in Fig. 1) were captured with a Leitz DMRB microscope with epifluorescence (Leica EL-6000) equipped with a specific filter for FG (Leica, A) and a digital Leica DFC 300 FX camera. Using Adobe Photoshop 7.0 (AdobeSystems, MountainView, CA, USA) pictures were flattened by subtracting background illumination and brightness and contrast were optimized. No further changes were performed. Finally, illustrations were designed with Adobe Photoshop 7.0 and Illustrator.

Results

For the description of the results we follow the cytoarchitecture and nomenclature by Paxinos and Franklin (2001) with a few modifications that are discussed where needed. For the amygdaloid complex (see Tables 1, 2), we follow the architecture proposed by Martínez-García et al. (2012) and the functional grouping of the chemosensory amygdala proposed by Gutierrez-Castellanos et al. (2010): olfactory nuclei, receiving inputs only from the main olfactory bulb (MOB); vomeronasal nuclei, receiving inputs only from the accessory olfactory bulb (AOB); and mixed nuclei, receiving inputs from both bulbs, with either olfactory or vomeronasal predominance.

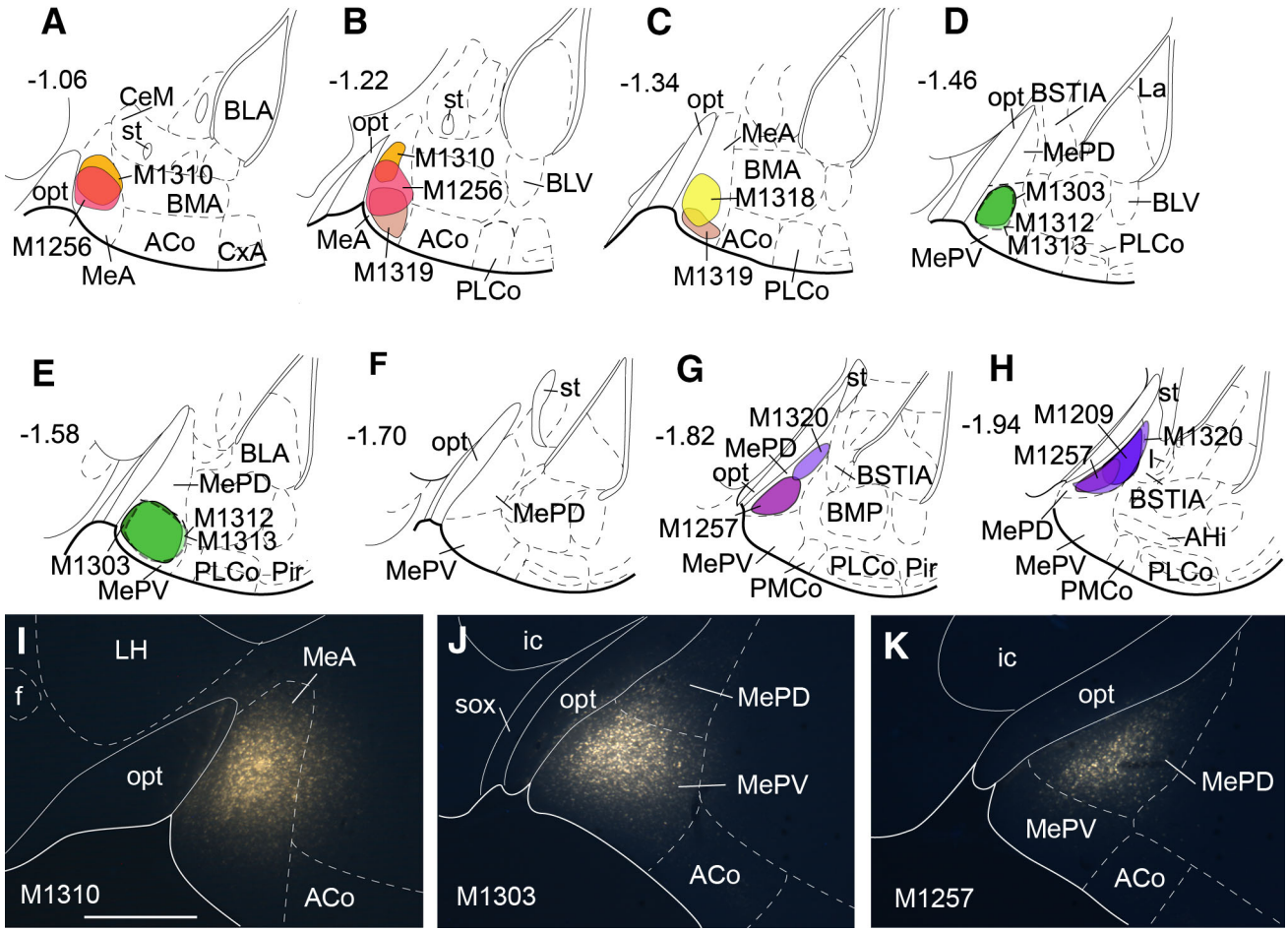

Fig. 1 Injection sites in the anterior, posteroventral and posterodorsal subdivisions of the medial amygdaloid nucleus in mice. **a**–**h** Schematic drawings representing the extent of the tracer injections in the anterior medial amygdaloid nucleus (*MeA*), posteroventral medial amygdaloid nucleus (*MePV*) and posterodorsal medial amygdaloid nucleus (*MePD*). The MeA injections are represented in panels **a**–**c**; MePV injections are shown in panels **d**, **e** (injections M1312 and M1313 were almost identical, and therefore one drawing illustrates both) and MePD injections are represented in panels **g**, **h**. Single injections are identified with the animal code. Note that no injection site is present in panel (**f**), shown only for the sake of the rostrocaudal continuity of the figure. **i**–**k** Fluorescent photomicrographs through the amygdala showing representative injections sites of fluorogold. **i** Injection site in MeA, case M1310. **j** Injection site in MePV, case M1303. **k** Injection site in MePD, case M1257. For abbreviations, see list. *Scale bar* in **i**, valid for *i*–*k* = 500 μm

Table 2 Semiquantitative rating of the density of the retrograde labelling resulting after tracer injections in three subnuclei of the medial amygdaloid nucleus

	MeA	MePV	MePD
Olfactory system			
Accessory olfactory bulb			
MiA rostral/MiA caudal	++++	++++	++++/++
Main olfactory bulb			
Mi	(+)[a]	0	(+)
Olfactory cortex			
DTT/VTT	++/+	+/0	−/0
Pir	++	+	(+)
DEn/VEn	++/++	++/+	+/(+)
Amygdala and BST			
Vomeronasal			
PMCo	++++	++++	++
Vomeronasal predominance			
MeA	**injection**	++++	++++
MeAV/MeAD	++++	+++/++	(+)/++
MePV	+++	**injection**	++++
MePD	++	+++	**injection**
BAOT	++++	++++	+++
AAV/AAD	++	++/+	(+)/(+)
Olfactory			
PLCo	+++	+++	++
APir	++	+	(+)
Olfactory predominance			
ACo	+++	+++	+++
CxA	++	+	0
LOT	+	(+)	+
Basolateral complex			
BLA	(+)	(+)	0
BLP	(+)	+	(+)
BLV	(+)	+	0
BMA	+++	++	++
BMP	+++	++	(+)
LaDL/LaVM/LaVL	(+)/+/+	(+)/+/(+)	0/0/0
Amygdalo-hippocampal transition area			
AHi	++	++	+++
Central			
CeC	0	(+)	0
CeL	(+)	0	0
CeM	+	+	+
I	+	+	(+)
IM	+	+	(+)
BSTL			
BSTLP	(+)	0	0
BSTLV	(+)	(+)	0
BSTM			
BSTMA	(+)	(+)	0
BSTMV	(+)	0	0
BSTMPM	++	++	++++
BSTMPI	+++	+++	++
BSTMPL	+	(+)	0
BSTIA	+++	++	++
Cortex and hippocampal formation			
Al	++	(+)	0
PrL	+	(+)	0
Cl	(+)	0	(+)
MO	+	+	(+)
LO	(+)	0	0
IL	+	(+)	(+)
DP	+	+	(+)
PRh	(+)	0	(+)
Hippocampal formation			
LEnt	++	+	+
CA1	+++	+++	++
S	++	++	+
Septum/striatum			
Lateral septal complex			
LSI	+	+	+
LSD	(+)	0	0
LSV	(+)	(+)	(+)
SHi	++	+	(+)
Medial septum/diagonal band			
MS	++	++	+
HDB/MCPO	++	+	+
VDB	++	+	(+)
Striato-pallidum			
VP	(+)	+	0
SL	+++	++	+
SI	++	++	+
IPAC	(+)	0	0
Thalamus			
PVA/PV	++/+	++/+	+/−
PVP	+++	+++	++
Re	++	++	+
MD	(+)	0	0
MHb	(+)	(+)	0
Zl	+	(+)	+
pv	+++	++	++
SPF	+++	++	++
SPFPC	++	++	++
PIL	+++	+++	+++
SG	++	+	(+)
PP	+++	+++	++
MGM	+	+	(+)
Hypothalamus			
Preoptic			

Table 2 continued

	MeA	MePV	MePD
MPA	(+)	0	(+)
MPO	+	+	++
LPO	(+)	0	(+)
Anterior			
AH	+	+	+
Pa	(+)	0	(+)
Tuberal			
VMH	++	++	+
DM	(+)	(+)	0
LH	+	+	+
Arc	(+)	0	(+)
TC	(+)	+	(+)
Mammilary			
PMD/PMV	0/+	0/+++	0/++++
SuM	(+)	+	(+)
PH	++	++	+
Brainstem and midbrain			
PAG	(+)	(+)	(+)
VTA	(+)	0	0
RLi	(+)	0	0
DR	+	+	+
IP	(+)	0	0
MnR	(+)	(+)	(+)
PB	++	++	+

[a] Retrograde labelling in the MOB is scarce in the injections not affecting significantly the superficial layer of the MeA, but moderate in the cases encompassing the superficial layer. ++++ very dense; +++ dense; ++ moderate; + scarce; (+) very scarce; 0 not found

Retrograde labelling with FG typically appears as granular staining of the cell body. Staining intensity ranged from a few granules surrounding the neuronal nucleus to darkly stained somata with labelling extending into the proximal dendritic tree. Each injection was photographed under fluorescence microscopy to map its location and extent (Fig. 1). In addition, retrograde labelling in structures adjoining the injection sites was analysed in fluorescence material, since it was difficult to discern in immunoperoxidase material.

Retrograde labelling after FG injections into the anterior subdivision of the medial amygdaloid nucleus (MeA)

Nine injections were aimed at the MeA, four of which were restricted to this subnucleus (see Fig. 1a–c, i). Five more injections were centred in the MeA but extended to some neighbouring structures such as the substantia innominata (M1242), the anterior amygdaloid area (M1248), the MePD (cases M1316 and M1314) or the MePV (M1317). The pattern of labelling was similar in all four restricted injections (case M1310 is illustrated in Fig. 2; but see below regarding labelling in the main olfactory bulb), and the labelling in non-restricted injections is fully consistent with the pattern described.

In general, the density of labelled cells was high in areas of the olfactory systems and in several nuclei of the amygdala and bed nucleus of the stria terminalis (BST), moderate in the hippocampal formation and scarce in the neocortex. Within the subcortical telencephalon, labelled cells were also present in the septum and basal forebrain. In addition, several populations of labelled cells were seen in several nuclei of the thalamus, hypothalamus as well as in some midbrain and brainstem centres.

Retrograde labelling in the olfactory system

As expected, injections of FG in the MeA gave rise to very dense retrograde labelling throughout the mitral cell layer of the accessory olfactory bulb (MiA) (Fig. 2a; Table 1), which represents one of the main sources of inputs to the MeA. In addition, the main olfactory bulb also displayed labelled mitral cells, mainly located in the medial and lateral aspects of the bulb (see Table 2). Labelling density in the MOB is relatively higher in case M1256, in which the injection is centred in the superficial layer of MeA, and in the non-restricted injection M1242, which involved the external layer of the MeA. By contrast, few labelled cells are present in the MOB of case M1310 (see Fig. 2a) in which the injection site was relatively deep and a small portion of layer 1 was involved.

Secondary olfactory centres also showed remarkable retrograde labelling. Thus, a moderate number of labelled cells was observed in the dorsal tenia tecta (DTT, layer III) (Fig. 3a), while the ventral tenia tecta (VTT) showed scarce labelling mainly located in its layer II. The piriform cortex (Pir) showed a heterogeneous pattern of retrograde labelling, from very scarce in the anterior Pir to dense in its caudal portion (Figs. 2b–j, 3d). Labelling was distributed in layers II and III but, occasionally, labelled cells were seen in layer I, just below the lateral olfactory tract (lo) (Fig. 2b–d). In addition, the endopiriform nucleus, especially its dorsal portion (DEn), also showed retrograde labelling, with a heterogenous antero-posterior distribution (Figs. 2b–j, 3d).

Retrograde labelling in the amygdala and BST

The amygdala (together with the BST) presented the densest populations of retrogradely labelled cells, and the most intensely labelled neurones. Labelling was present in the chemosensory nuclei, as well as in deep nuclei

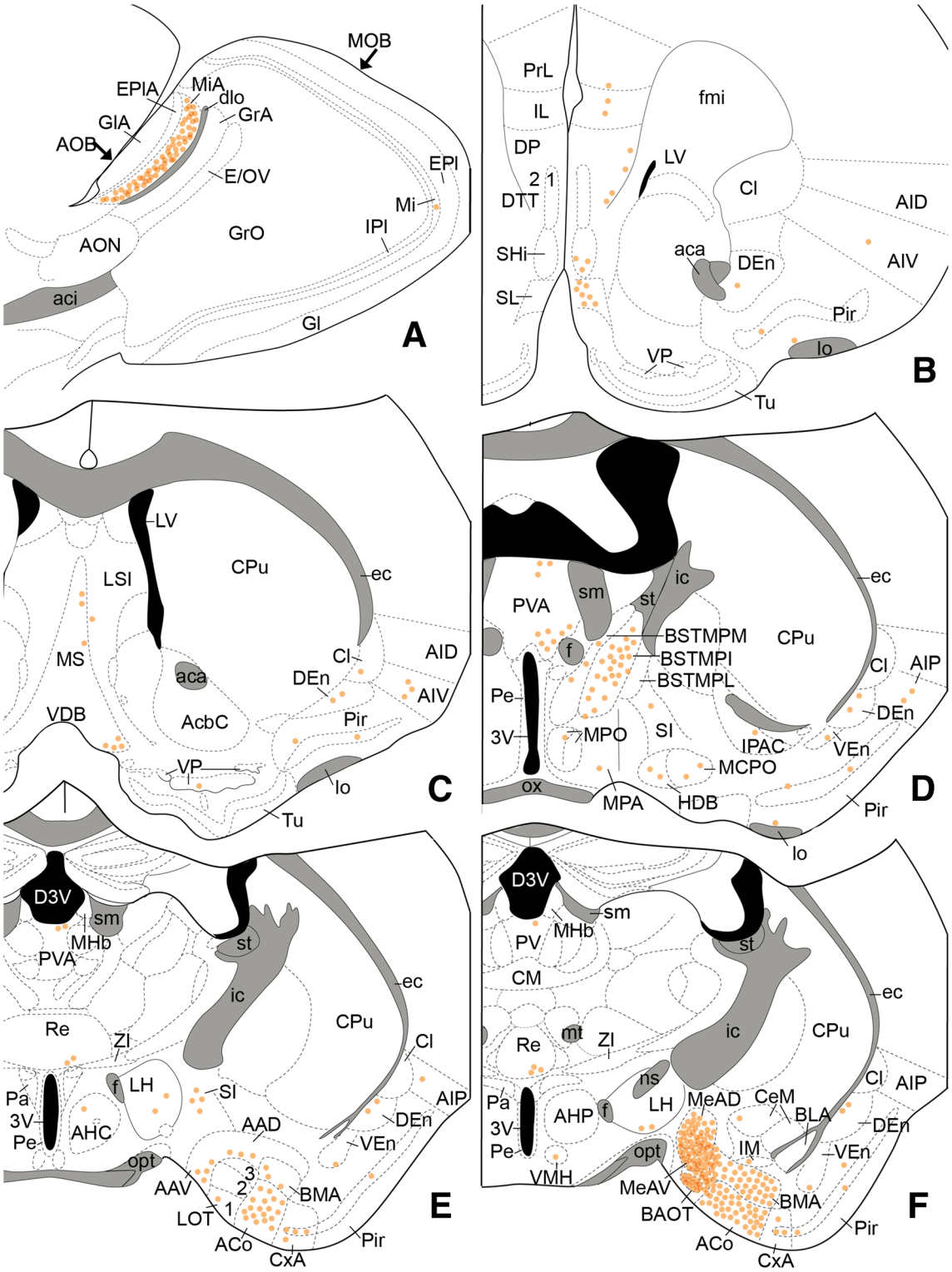

Fig. 2 Semi-schematic drawings of parasagittal (**a**) and frontal (**b–l**) sections through the mouse brain showing the distribution of retrogradely labelled somata following a fluorogold tracer injection in the anterior medial amygdaloid nucleus. The injection site is depicted in panel (**g**). The semi-schematic drawings are based on the case M1310, which presented the largest restricted injection. Despite being relatively large, this injection was centred in deep layers of the MeA and the injection site only encompassed the superficial layer 1 marginally. Accordingly, labelling in the main olfactory bulb (**a**) is much scarcer then in other injections in the MeA. **b** Is rostral, **l** is caudal. For abbreviations, see list

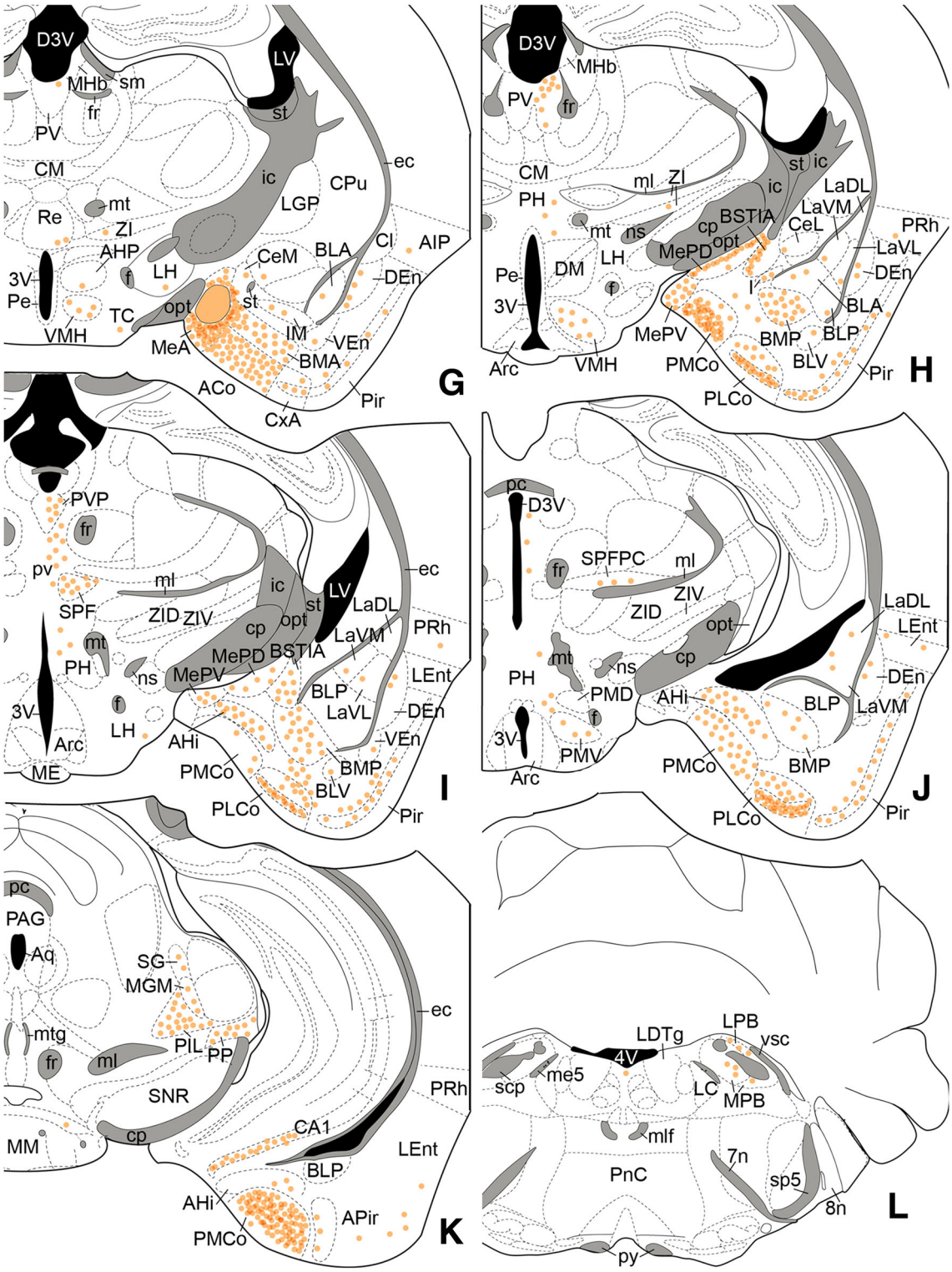

Fig. 2 continued

belonging to the basolateral/amygdalo-hippocampal or central divisions.

Within the chemosensory amygdala, labelling was dense in the PMCo (Fig. 2h–k), the only vomeronasal nucleus that does not receive direct olfactory projections. In general, this nucleus showed a very dense labelling, with labelled somata located in the cellular layers (layers II and III). Retrogradely labelled neurones appeared

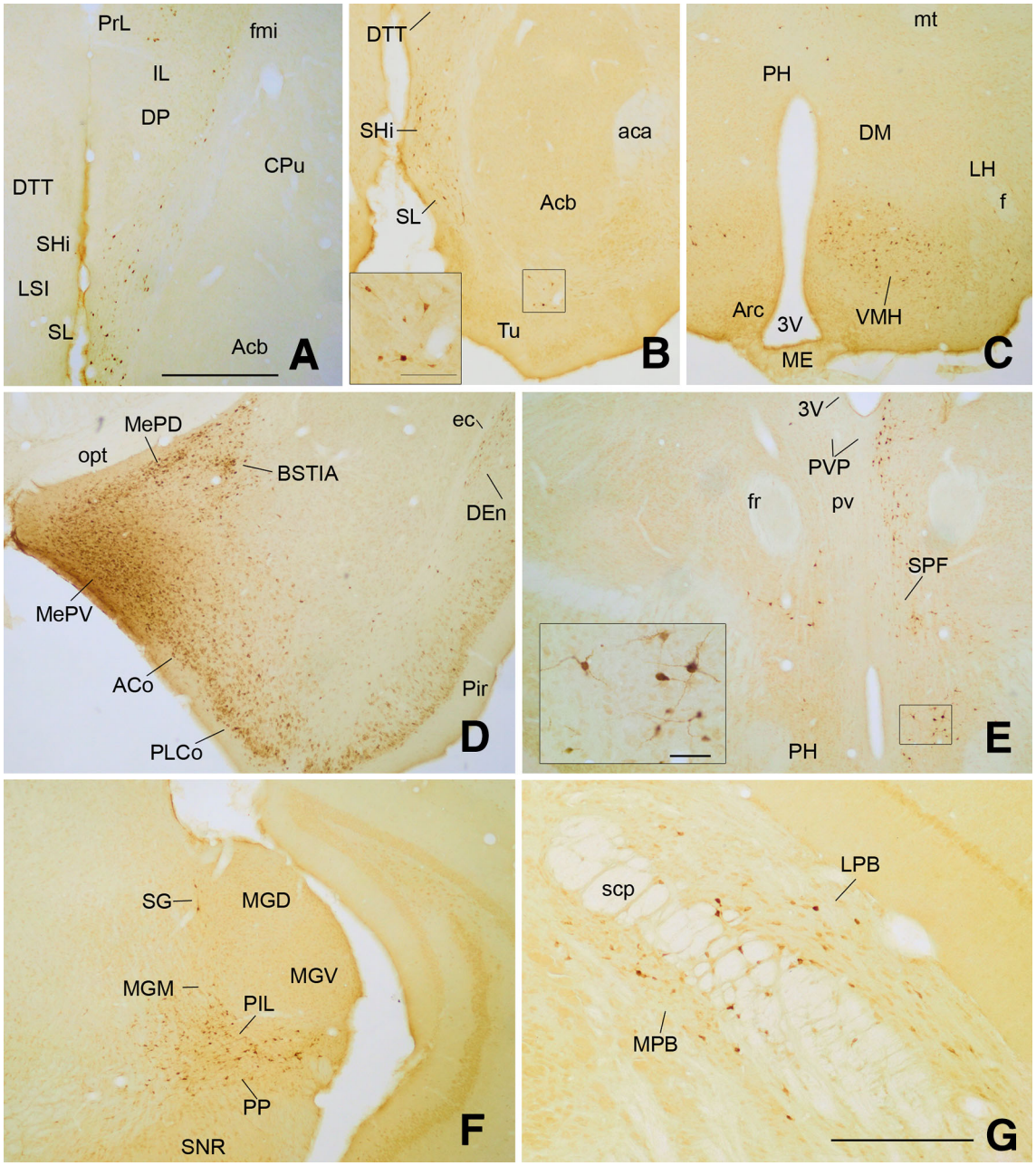

Fig. 3 Photomicrographs of frontal sections illustrating the retrograde labelling through the mouse brain of animals receiving a fluorogold injection in the anterior medial amygdaloid nucleus. The images correspond to the retrograde labelling presented in the cases M1310 (**a**, **b**, **c**, **f**) and M1319 (**d**, **e**, **g**). **a** Retrograde labelling in the prelimbic and infralimbic areas of the prefrontal cortex and the rostral areas of the septum. **b** Retrogradely labelled neurones in the boundary between the deep olfactory tubercle and the nucleus accumbens. **c** Retrogradely labelled neurones in the ventromedial hypothalamus. **d** Numerous labelled cells in the posterodorsal and posteroventral subnuclei of the medial amygdala, as well as in the anterior and posterolateral cortical amygdaloid nuclei. **e** Retrogradely labelled cells in the midline thalamus and posterior hypothalamus. The inset shows the Golgi-like stained neurones observed in the posterior hypothalamic area. **f** Retrogradely labelled neurones in the posterior intralaminar thalamic complex. **g** Retrograde labelling in the parabrachial nucleus of the brainstem. For abbreviations, see list. *Scale bar* in **a** (valid for **b**–**f**): 500 μm. *Scale bar* in **g**: 250 μm. *Scale bar* in *inset* in **b**: 100 μm. *Scale bar* in *inset* in **e**: 50 μm

heterogeneously distributed: labelling was very dense in the rostral PMCo (adjacent to the MePV, Fig. 2h), moderate in intermediate levels, where labelled cells were located mainly in the lateral aspect of the nucleus (Fig. 2i, j), and very dense in the caudal edge of the nucleus (Fig. 2k).

With regard to the mixed chemosensory amygdala, within the nuclei with vomeronasal predominance,

labelling was present in the different divisions of the Me, the bed nucleus of the accessory olfactory tract (BAOT) and the anterior amygdaloid area (AA) (Table 2). Within the Me very dense labelling was observed in the non-injected portions of the MeA, including the dense-celled regions of the anteroventral (MeAV) and the anterodorsal (MeAD) parts of the MeA, which are rostral to the injection site (Fig. 2f). The MePV showed a heterogeneous pattern of labelling along its antero-caudal axis, very dense at rostral levels (Fig. 3d) and less so caudally (Fig. 2h, i). Finally, the MePD presented, in general, moderate labelling with a conspicuous heterogeneity in the distribution of labelled cells (Fig. 2h, i). As Fig. 3d illustrates, at least at rostral levels of the MePD, labelled cells apparently lined up the outer boundary of the cell layer, with deeper regions showing a lower density of stained cells. In addition, the BAOT showed also very dense labelling with darkly stained somata (Fig. 2f), whereas the ventral and dorsal divisions of the AA (AAV, AAD) presented a moderate density of retrograde labelling.

Regarding to the olfactory amygdala (Table 2), the posterolateral cortical amygdaloid nucleus (PLCo) displayed a high density of labelled cells (Fig. 2h–j), most cells being located in layer II and to a lesser degree in layer III (see Fig. 3d). By contrast, the amygdalo-piriform transition area (APir) showed a moderate density of labelled cells (Table 2; Fig. 2k).

Among the nuclei of the mixed chemosensory amygdala with olfactory predominance (Table 2), the anterior cortical amygdaloid nucleus (ACo) showed a dense population of labelled neurones in the cell layer (Figs. 2e–g, 3d). The cortex-amygdala transition zone (CxA) displayed moderate labelling density, with the labelled somata mainly located in layer II (Fig. 2e). Finally, the nucleus of the lateral olfactory tract (LOT) showed just a few retrogradely labelled cells confined to layer I (Fig. 2e).

Within the multimodal or deep amygdala (Table 2), in the basolateral complex, the anterior and posterior parts of the basomedial amygdaloid nucleus (BMA, BMP, respectively) showed a heterogeneous labelling density (dense, in average). In both nuclei dense labelling was present in their rostral parts while in their posterior parts the labelling decreased to moderate (Fig. 2e–j). In the basolateral amygdaloid nucleus, the anterior (BLA), ventral (BLV) and posterior (BLP) parts showed scarce labelling (Fig. 2h–k). In the lateral amygdaloid nucleus labelling was scarce in its ventromedial and ventrolateral parts (LaVM, LaVL) and very scarce in its dorsolateral part (LaDL) (Fig. 2h–j). Finally, in the amygdalo-hippocampal area (AHi) labelling was denser in the rostral half than its caudal aspect (Fig. 2i–k).

To complete the description of retrograde labelling in the amygdala, scarce or very scarce labelling was observed in the central amygdaloid nucleus (Table 2), mainly in its medial division (CeM, Fig. 2f–h), and in the intercalated nuclei of the amygdala (I), including the main intercalated nucleus (IM; Fig. 2f–h).

Within the BST complex, the posterior part of the medial subdivision presented the strongest labelling (Fig. 2d). The posterointermediate part of the medial division of the BST (BSTMPI) showed dense labelling whereas in the posteromedial (BSTMPM) and posterolateral (BSTMPL) parts labelled cells were relatively scarcer (Fig. 4a, d). Other parts of the BST (results not shown) display a low number of labelled cells, including the ventral (BSTMV) and anterior parts of the medial BST (BSTMA), and the posterior and ventral parts of the lateral BST (BSTLP and BSTLV, respectively; Table 1). Finally, the intraamygdaloid part of the BST (BSTIA) showed dense labelling with the stained cells located more frequently in its medial aspect adjoining the MePD (Figs. 2h, i, 3d).

Retrograde labelling in the cerebral cortex, including the hippocampal formation

According to (Palomero-Gallagher and Zilles 2015), the cerebral cortex is composed of isocortical areas showing 6 cell layers, and several allocortical regions with 1 (hippocampal formation, archicortex) or 2 cell layers (primary olfactory cortex). The isocortex and allocortex are separated by stepwise transition zones known as mesocortex. After injections in the MeA, retrograde labelling was absent in the isocortex, scarce in the transitional mesocortical areas, prominent in some areas of the hippocampal formation and even abundant in paleocortical areas (see above). Thus, a low density of retrogradelly labelled cells was observed in regions of the prefrontal cortex, including the medial orbital (MO), prelimbic (PrL), infralimbic (IL) and dorsal peduncular cortices (DP) (Figs. 2b, 3a; Table 2). Except for case M1257, in which the IL displayed a moderate number of labelled cells, the rest of the areas in the medial prefrontal cortex showed very scarce labelling. In the lateral aspect of the mesocortex, few labelled cells were observed in the lateral orbital cortex (LO), a moderate density of labelled cells appeared in the agranular insular cortex (ventral and posterior parts; AIV, AIP) and scarce labelling was present in the perirhinal cortex (PRh) (Fig. 2c–k). In addition, a few retrogradelly labelled neurones were occasionally observed in the claustrum (Fig. 2c), a cortical derivative (Puelles et al. 2000) located deep to the insula.

More caudally, a moderate number of labelled neurones were seen in the lateral entorhinal cortex (LEnt; Fig. 2i–k), where labelling was especially dense immediately caudal to the APir.

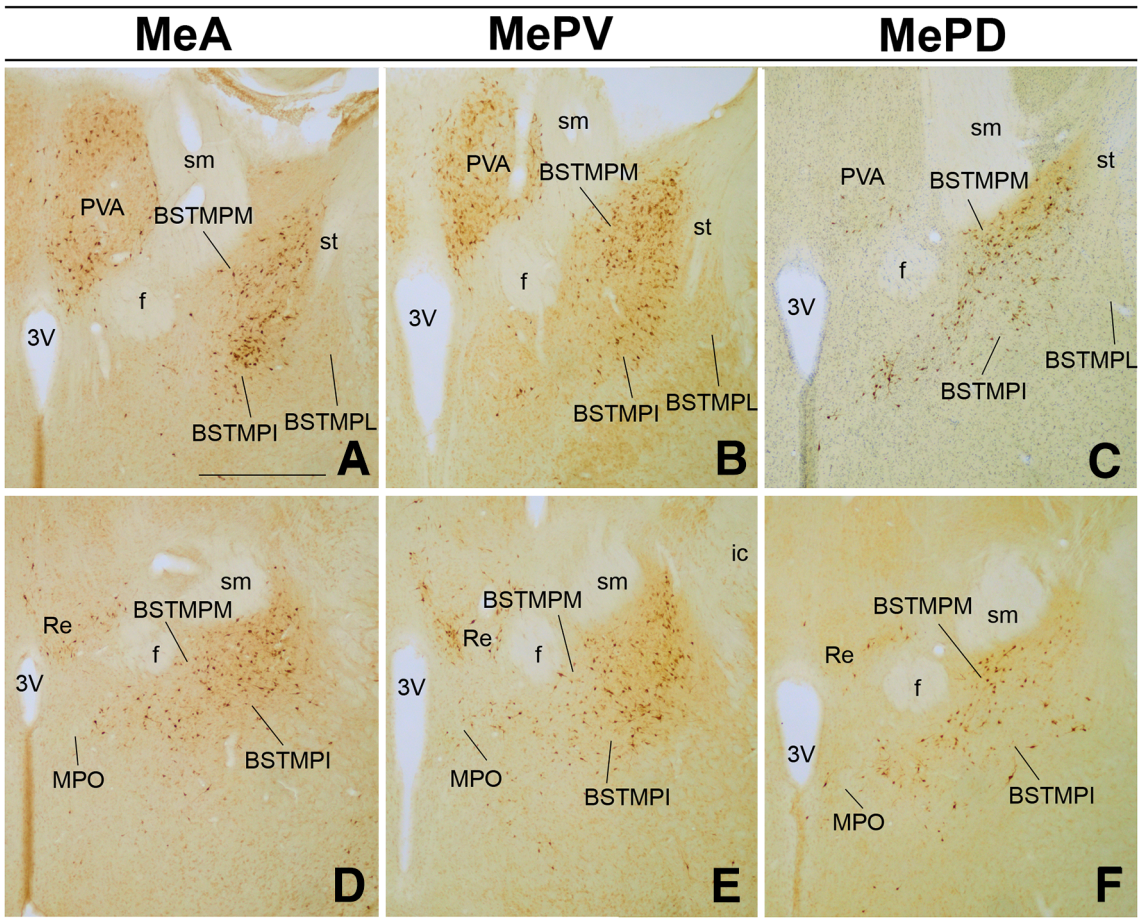

Fig. 4 Photomicrographs of frontal sections illustrating the retrograde labelling present in the medial subdivision of the bed nucleus of the stria terminalis (*BSTM*) after fluorogold injections in the medial amygdaloid nucleus. **a**, **d** Retrograde labelling after an injection in the anterior part of the medial amygdala, case M1318, showing the resulting dense labelling in the posterointermediate part of the BSTM (**a** is rostral, **d** is caudal). **b**, **e** Retrograde labelling after an injection in the posteroventral part of the medial amygdala, case M1303, illustrating the dense labelling observed in the posterointermediate part of the BSTM and the heterogeneous labelling present by the posteromedial part of the BSTM (**b** is rostral, **e** is caudal). **c**, **f** Retrograde labelling after an injection in the posterodorsal part of the medial amygdala, case M1257, illustrating the dense labelling showed by the posteromedial part of the BSTM (**c** is rostral, **f** is caudal). Note also the dense labelling in the anterior paraventricular thalamic nucleus in **a** and **b**. For abbreviations, see list. *Scale bar* in **a** valid for (**b**–**f**): 500 μm

Finally, regarding the hippocampus, a dense population of labelled somata appeared restricted to the ventralmost region of the field CA1 of the caudal hippocampus (CA1) (Fig. 2k).

Labelling in the septum and ventral forebrain

In the septal complex, a moderate density of labelling appeared in the rostral septohippocampal nucleus (SHi), just ventral to the DTT (Figs. 2b, 3a). The intermediate part of the lateral septum (LSI) displayed scarce labelling, with the labelled somata located next to the medial septal nucleus (MS) (Fig. 2b, c). In the rest of the complex, we observed very scarce labelling in the dorsal and ventral part of the lateral septum (LSD, LSV, respectively).

The vertical and horizontal limb of the diagonal band (VDB, HDB, respectively) and the MS presented a moderate number of labelled somata lining up at the boundary with the LSI (Fig. 2c). At the rostral HDB, labelled somata clustered in the lateral edge of the HDB, next to the olfactory tubercle (Tu; Fig. 2c). In contrast, more caudally intensely labelled somata were distributed homogeneously in the caudal HDB and adjacent magnocellular preoptic nucleus (MCPO; Fig. 2d). Within the basal cerebral hemispheres, at rostral levels a number of darkly stained cells were observed in the territory located between the nucleus accumbens (Acb) and the Tu (Fig. 3b). In addition, a group of intensely labelled cells was observed in the semilunar nucleus (SL; Figs. 2b, 3a). Finally, the substantia innominata (SI) presented moderate labelling, and the

ventral pallidum (VP) and interstitial nucleus of the posterior limb of the anterior commissure (IPAC) showed a few, scattered labelled somata (Fig. 2c–e).

Retrograde labelling in the thalamus

After FG injections in the MeA, retrograde labelling was observed in the anterior, midline and posterior-intralaminar-peripeduncular thalamic regions. Within the anterior thalamus the paraventricular thalamic nucleus (PVA) displayed a large number of labelled cell bodies (Figs. 2d, e, 4a), with a very striking heterogeneous distribution (Table 2). In its rostral edge, it presented a very dense labelling with darkly stained cells. At intermediate rostrocaudal levels, the labelling decreased to scarce (Fig. 2e–g), and even more caudally, the posterior paraventricular thalamic nucleus (PVP) showed a high density of intensely labelled cells (Figs. 2h, i, 3e).

In addition, a low density of labelled cells could be observed in the mediodorsal nucleus (MD) and medial habenula (MHb). In one injection (M1256), the central medial thalamic nucleus and the lateral habenular nucleus also showed a few labelled cells. Ventrally, a group of labelled neurones appeared in nucleus reuniens (Re; Figs. 2e–g, 4d) and the zona incerta (ZI) also showed a few labelled cell bodies (Fig. 2f, g).

In the caudal thalamus, dense retrograde labelling appeared in the SPF, and a group of labelled cells appeared near the midline, among the tracts of the pv, apparently connecting the cell groups in the PVP and SPF (Figs. 2i, 3e). Within the SPF, a small group of labelled cell bodies extended caudo-laterally into its parvocellular part (SPFPC; Fig. 2j). Even more caudally, a high density of retrogradely labelled cells was seen in the posterior intralaminar (PIL) and peripeduncular nucleus (PP). Retrogradely labelled cells appeared also in the medial division of the medial geniculate nucleus (MGM) (Figs. 2k, 3f) and the suprageniculate nucleus (SG), where labelling was scarcer.

Retrograde labelling in the hypothalamus

In the hypothalamus labelled cells were present from preoptic to mammillary levels, but their density was quite low with two exceptions, the ventromedial hypothalamic nucleus (VMH) and the posterior hypothalamic nucleus (PH).

In the preoptic hypothalamus, sparse labelled neurones were present in the medial preoptic nucleus (MPO) and the medial and lateral preoptic areas (MPA, LPO; Fig. 2d; Table 2). At anterior levels, sparse labelled cell bodies were seen in the anterior hypothalamic area (AH) and paraventricular hypothalamic nucleus (Pa). At tuberal levels the VMH showed a moderate number of labelled cells (Fig. 2g, h) bilaterally, with clear ipsilateral dominance, present both in its dorsolateral and ventrolateral divisions (Fig. 3c). In addition, sparse labelled cells appeared in the dorsomedial (DM) and arcuate nucleus (Arc), in the tuber cinereum (TC) and in the lateral hypothalamic area (LH; Figs. 2e–i, 3c).

Within the mammillary hypothalamus, labelled cells were present in the PH (Fig. 2h–j), mainly at at caudal levels. In addition, retrograde labelling was scarce in the ventral premammillary nucleus (PMV). Finally, the supramammillary nucleus (SuM) displayed a few, sparse retrogradely labelled cells (Fig. 2k).

Retrograde labelling in the midbrain and brainstem

Labelled cells were very scarce and scattered in diverse nuclei of the midbrain and brainstem, including the ventral tegmental area (VTA), interpeduncular nucleus (IP), periaqueductal gray (PAG), rostral linear nucleus of the raphe (RLi) and the dorsal (DR) and median raphe nuclei (MnR) (Table 2). The few retrogradely labelled cells found in the PAG were scattered across its different subdivisions. In addition, the parabrachial nucleus (PB) presented a moderate density of labelled cells, both in its medial and lateral divisions (Figs. 2l, 3g).

Contralateral labelling

Although FG injections in the MeA gave rise mainly to ipsilateral retrograde labelling, labelled cells were also observed in the side of the brain contralateral to the injection. In general, these nuclei were the contralateral counterparts of the ipsilateral structures that presented very dense or dense labelling. Thus contralateral labelling was scarce in the amygdaloid PLCo and PMCo, the thalamic SPF, PIL and PP, the VMH in the hypothalamus and the PB in the brainstem. Occasional (very scarce) labelling was also observed in the contralateral LEnt, in the hippocampal formation; the LSI, VDB, and HDB in the septal complex; the SL and SI in the striato-pallidum; numerous structures in the amygdala and BST (MeA, BLA, BMP, APir, BSTMPM, BSTMPI); the PVA, Re, ZI, pv and SPFPC in the thalamus; the MPO, Pa, PH, PMV and Arc in the hypothalamus; and the PAG, AH and DR in the midbrain and brainstem.

Retrograde labelling after FG injections into the posteroventral subdivision of the medial amygdaloid nucleus (MePV)

Six injections of FG involved the MePV, three of which were restricted to this subnucleus (cases M1303, M1312 and M1313; Fig. 1d, e, j) and the remaining encompassed

also adjoining regions such as the caudal MeA (M1249), the ventral MePD (M1259) and the ACo and PMCo (M1301). The results of non-restricted injections are consistent with the pattern of labelling revealed by restricted cases, which is described below.

Experiment M1303 is illustrated as representative case of retrograde transport of FG from the MePV (Fig. 5). In general, retrograde labelling was present in the same nuclei observed after FG injections in the MeA. Differences pertained to the relative density of labelled cells and their distribution within the nucleus in some centres of the olfactory systems, cortex, septum, striato-pallidum, thalamus and hypothalamus (see Table 2). Therefore, we will focus our description on those differences.

Retrograde labelling in the olfactory system

As in the case of FG injections in the MeA, very dense labelling was observed throughout the MiA of the AOB (Figs. 5a, 6a). In contrast, no labelling appeared in the MOB.

Among the secondary olfactory centres, the observed retrograde labelling was in general less dense than after the injection in the MeA. Thus, the DTT and anterior Pir presented scarce labelling (Fig. 5b–d), and only in the caudal part of the Pir (next to the PLCo), we observed a moderate density of retrogradely labelled cells (mainly in layer II, Fig. 5h, j). Similar to the Pir, the DEn showed scarce labelling in its rostral part and moderate labelling caudally (Fig. 5c, j). Last of all, the VEn showed moderate labelling (Fig. 5d, j).

Retrograde labelling in the amygdala and BST

Within the vomeronasal amygdala, as described in the injections in the MeA, the PMCo showed in general a very dense labelling with darkly stained somata (Table 2). The intranuclear distribution of labelled stomata was heterogeneous (although not as conspicuous as in the case of MeA injections), with labelling being dense rostrally and caudally but moderate at intermediate levels (Figs. 5j, k, 6d).

Regarding to the mixed nuclei with vomeronasal predominance (Table 2), the MeA showed also a very dense labelling (Figs. 5h, 6c). Within the MeA, the labelling presented a heterogeneous distribution, with moderate and dense labelling observed in the MeAD and MeAV, respectively (Figs. 5g, 6b). The MePD showed in general a dense labelling (Table 2), with a heterogeneous distribution of labelled somata (Fig. 5i, j). Darkly stained somata were aligned along the most medial part of the cellular layer in the limit with the external layer. The inner part of the cellular layer presented moderate labelling (which was denser than that observed in the same location after the MeA injections) (Fig. 5i, 2h respectively). In addition, the BAOT presented very dense labelling (Figs. 5g, 6b) and the AAV and AAD, showed moderate and scarce labelling, respectively (Fig. 5e, f).

Within the olfactory amygdala (including the mixed nuclei with olfactory predominance) the retrograde labelling observed was very similar to that obtained following the injection in the MeA (Table 2). Thus, the PLCo (Fig. 5i, j) and ACo (Figs. 5f–i, 6b, c) presented dense labelling, while the APir (Fig. 6d) and CxA (Fig. 5e–h) showed scarce labelling. Finally, in the LOT we observed very scarce labelling with the labelled neurones present in layer I (Fig. 5f).

Within the basolateral complex, the BMA and BMP showed in general a moderate labelling (Table 2) with a heterogeneous distribution. In the BMA the labelling was mainly located in its anterior part (Fig. 5f–i), whereas in the BMP retrogradely labelled cells were more frequent in its posterior aspect (Fig. 5i–k). Within the lateral amygdaloid nucleus, the LaVM presented scarce labelling and only a few cells were present in the LaDL and LaVL (Fig. 5i, j). Retrograde labelling was also scarce in the basolateral nucleus, where it was mainly observed in the BLP and BLV (Fig. 5h–k).

With regard to the AHi, as observed following MeA injections, it showed a moderate amount of labelling (Table 2), present mainly in its rostral part (Fig. 5j, k).

Finally, the central amygdala and associated intercalated cell masses showed almost the same pattern of retrograde labelling that we observed following the MeA injections (Table 2), with only a few labelled cells observed mainly in the CeM, the IM and I (Fig. 5f–h; Table 2).

The labelling obtained in the BST followed the same pattern described after the injections in the MeA (Table 2). The densest labelling was present in the BSTMPI (Figs. 4b, e, 5d, e), and a moderate density of labelled cells was observed in the BSTMPM (Figs. 4b, e, 5d, e). In addition, very scarce labelling was present in the BSTMA and the BSTLV (Table 2). Finally, the BSTIA showed a moderate amount of retrogradely labelled cells, with darkly stained somata located along its limit with the MePD (Fig. 5i).

Retrograde labelling in the cerebral cortex, including the hippocampal formation

In general, the retrograde labelling resulting from the MePV injections was less dense than the one observed in the MeA injections (Table 2). Scarce retrogradely labelled cells were present in the MO and DP, with only a few cells observed in the IL, PrL and AI (Fig. 5b–k). Within the hippocampal formation, the CA1 showed dense labelling, with the labelled cells restricted to its ventral part (Fig. 6d). By contrast, the LEnt presented scarce labelling (Fig. 5j, k).

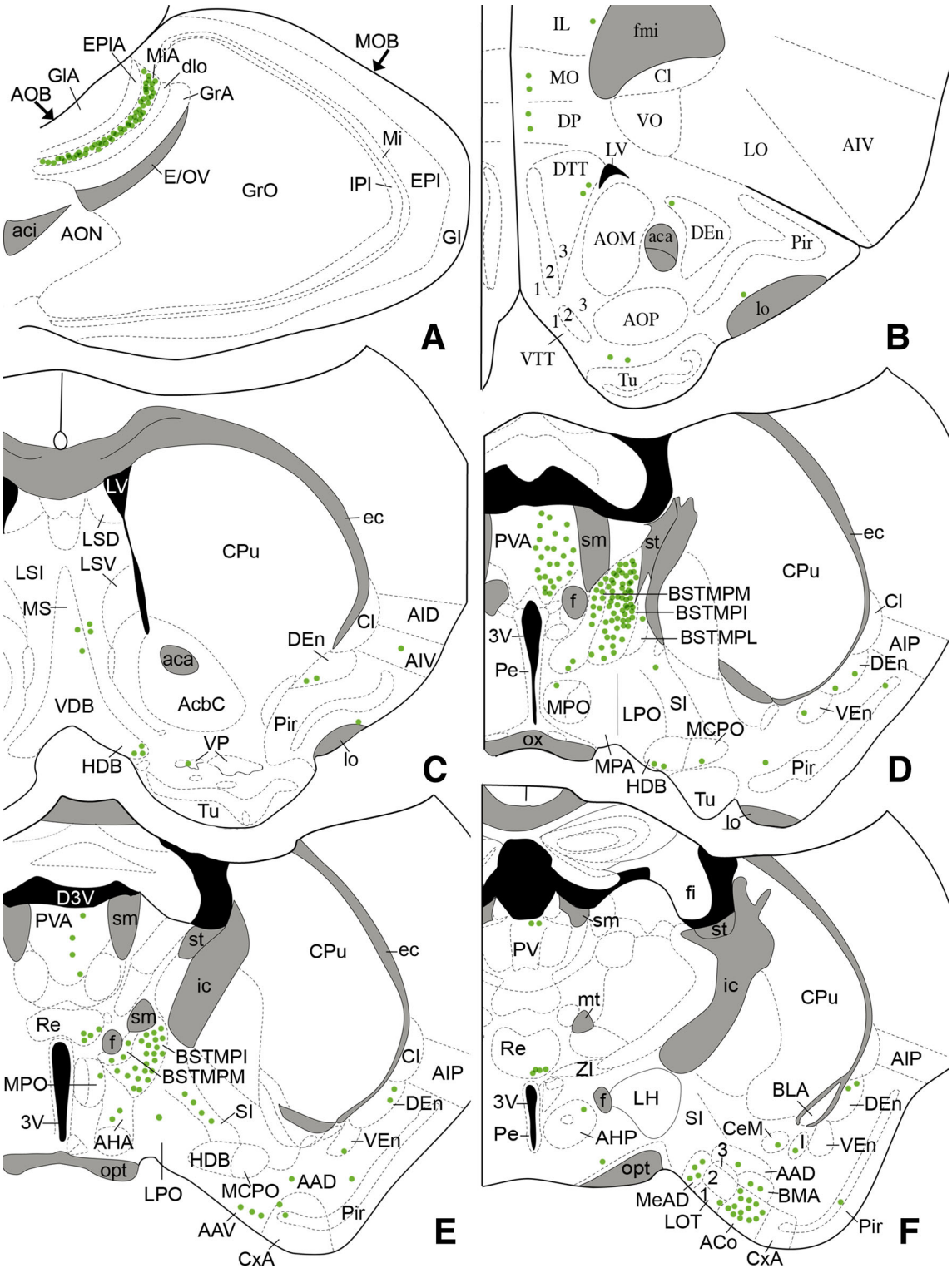

Fig. 5 Summary of the distribution of retrograde labelling following a fluorogold injection in the posteroventral medial amygdaloid nucleus, plotted onto semi-schematic drawings of parasagittal (**a**) and frontal (**b**–**l**) sections through the mouse brain. The injection site is depicted in panel (**i**). **a** Is rostral, **l** is caudal. The semi-schematic drawings are based on the case 1303, which presented the largest restricted injection. For abbreviations, see list

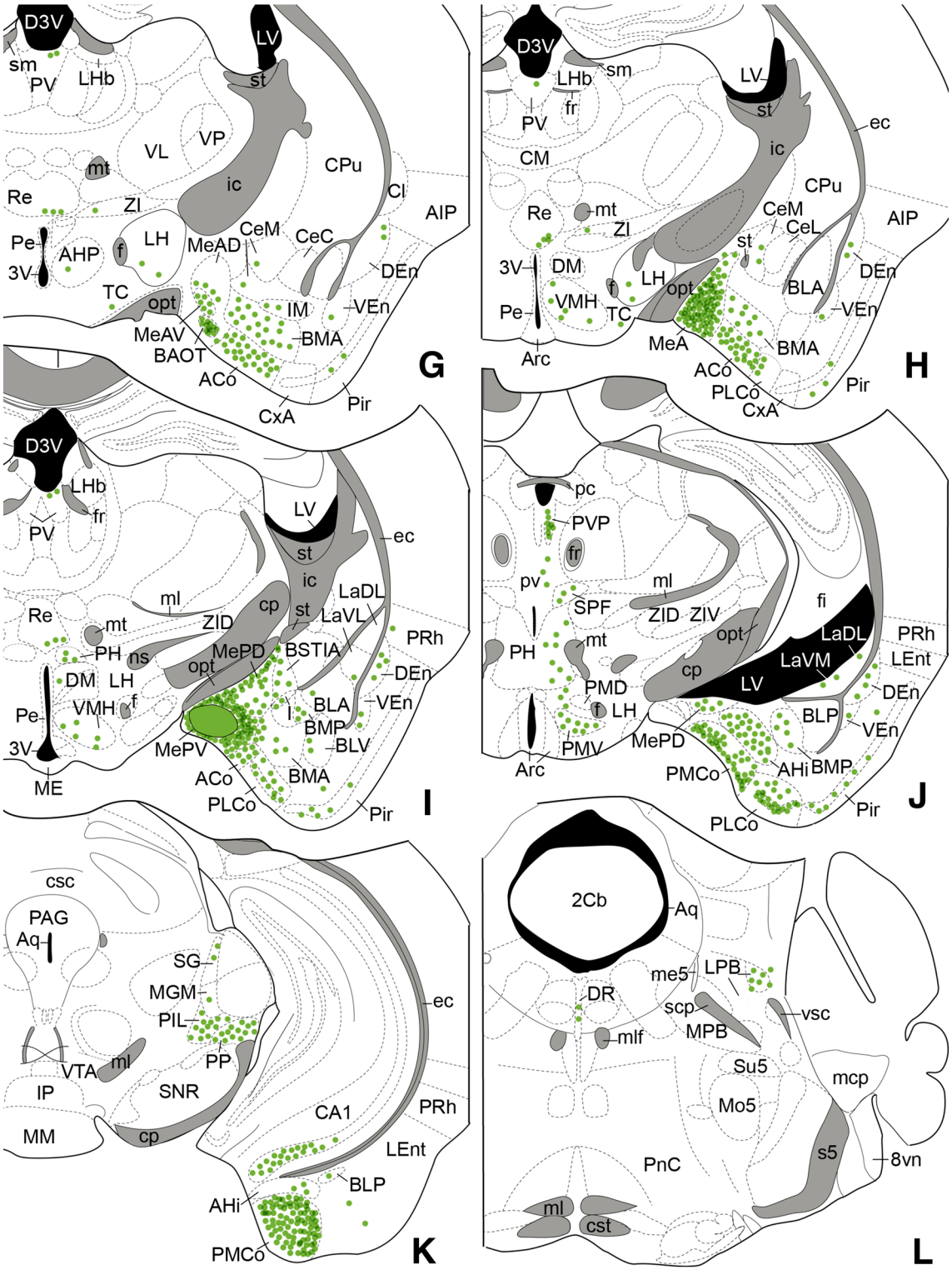

Fig. 5 continued

Labelling in the septum and ventral forebrain

As described for the cortex, the septum and striatum showed less retrograde labelling than that observed after the MeA injections (Table 2). The SHi presented scarce labelling (Table 2), with darkly stained somata mainly clustered dorsal to the SL (as shown in the MeA injections, see Fig. 3a). The LSI and LSV showed scarce or very

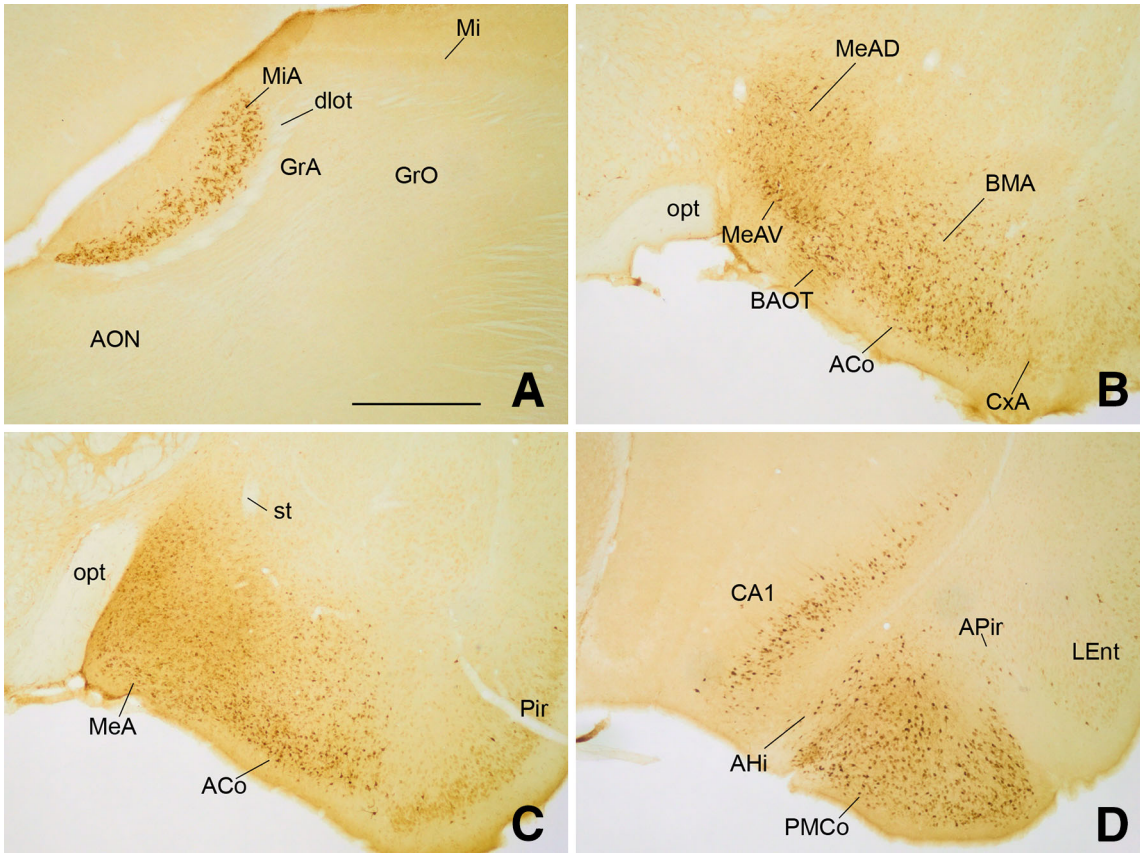

Fig. 6 Photomicrographs of parasagittal (**a**) and frontal (**b–d**) sections through the mouse telencephalon, illustrating the retrograde labelling observed in animals receiving a fluorogold injection in the postero-ventral medial amygdaloid nucleus. The images correspond to the retrograde labelling presented in the cases M1313 (**a**, **d**) and M1303 (**b**, **c**). **a** Retrogradely labelled mitral cells in the accessory olfactory bulb. **b** Numerous labelled cells in the anterodorsal and anteroventral subdivisions of the anterior medial amygdaloid nucleus, as well as in the bed nucleus of the accessory olfactory tract, the anterior cortical amygdaloid nucleus and the basomedial nucleus. **c** Very dense retrogradely labelled cells in the anterior medial amygdaloid nucleus, just rostral to the injection site. **d** Retrogradely labelled cells in the posteromedial cortical amygdaloid nucleus and in the ventral hippocampus. For abbreviations, see list. *Scale bar* in **a** (valid for **b–d**): 500 μm

scarce labelling respectively (Fig. 5c; Table 2). No labelling appeared in the LSD.

In the MS, VDH and HDB/MCPO, the location and distribution of the labelled somata were similar to that previously described for the MeA injections (see description above). The main difference was a relatively scarcer number of labelled cells in the diagonal band (Fig. 5c–e).

In the rostral striato-pallidum, as described in the MeA injections, a group of darkly stained somata was located between the Tu and the Acb (Fig. 5b). In addition, the SL presented moderate labelling (Table 2), with some darkly stained cells. More caudally, a few labelled cells were present in the VP (Fig. 5c). Finally, the SI showed also moderate labelling (Fig. 5d–f).

Retrograde labelling in the thalamus

The PVA, PV, PVP and Re showed the same densities and distribution of retrograde labelling described in the MeA injections (see description above, Table 2). Briefly, the PVP and PVA showed dense and moderate labelling, respectively, with only scarce labelling observed at intermediate levels (PV) between the PVA and the PVP (Figs. 4b, e, 5d–j). The Re presented a moderate number of retrogradely labelled cells.

Regarding to the structures of the posterior intralaminar thalamus (SPFPC, PIL, PP and MGM), all showed the same densities of labelling, distribution of labelled somata, and presence of darkly stained somata as described in the MeA injections (see the description above, Table 2). In summary, the PIL and PP showed dense labelling, the SPFPC presented moderate labelling and only a few labelled cells were present in the MGM (Fig. 5j, k).

Retrograde labelling in the hypothalamus

The VMH, MPO, AH, LH and DM presented the same densities of retrograde labelling (Table 2) and distribution

of labelled somata previously described for the MeA injections (see description above). Briefly, the VMH showed moderate labelling. In the MPO, AH and LH we observed scarce labelling, and only very few cells appeared in the DM (Fig. 5d–j).

The most relevant difference with the retrograde labelling observed after the injection in the MeA is the dense labelling with darkly stained somata present in the PMV of the mammillary hypothalamus (Fig. 5j; Table 2). We also observed minor differences in the PH, SuM and TC. In the case of the PH, the labelling was moderate (as in the MeA injections) but labelled cells were strikingly clustered ventrally to the pv and dorsally to the PMD (Fig. 5i, j; Table 2).

Retrograde labelling in the midbrain and brainstem

The PB showed a moderate density of labelled cells with the somata mainly located between its rostral part and the beginning of the fourth ventricle (Fig. 5l). In addition, the DR presented a low number of retrogradely labelled cells (Fig. 5l) and only very scarce labelling was present in the PAG and the MnR (Table 2).

Contralateral labelling

As described in the injection in the MeA, the retrograde labelling resulting from the MePV injections was mostly ipsilateral, although some structures showed bilateral labelling. We observed moderate labelling in the contralateral PMCo, and scarce labelling in the PIL, PP, VMH and PB. In addition, we observed very scarce labelling in several amygdaloid structures (MeA, MePV, AVV, ACo and BMA), in some BST subnuclei (BSTMPM and BSTMPI), in the hippocampal CA1, in the septum and ventral forebrain (LSI, MS, HDB, VDB, SL and SI), in the thalamus (PVA, PV, PVP, pv, Re, ZI, SPF and SPFPC), in the hypothalamus (MPO, LH, Arc and PH) and finally in the PAG and MnR of the midbrain and brainstem.

Retrograde labelling after FG injections into the posterodorsal division of the medial amygdaloid nucleus (MePD)

We obtained six injections in the MePD, three of them (cases M1209, M1257 and M1320) restricted to this subnucleus (Fig. 1g, h). All these injections affected the cellular layer of the caudal half of the MePD. Case M1257 (Fig. 1k) was used to illustrate the observed retrograde labelling throughout the brain (Fig. 7). The non-restricted injections affected adjoining structures, such as the MePV (case M1307), the MeA (case 1308) or the BMA (case M1307), but were useful to corroborate the observed labelling.

The three restricted injections gave rise to a similar pattern of retrograde labelling, described below and summarized in Table 2. In general, a smaller number of neural structures presented labelling and they showed less density of labelled cells compared with the MeA and MePV injections. Differences were mainly observed in the AOB and some centres of the amygdala, BST and hypothalamus (see Table 2). We will focus our description on those differences.

Retrograde labelling in the olfactory system

In contrast to the results obtained following the injections in the MeA and MePV, the retrograde labelling observed in the AOB was strikingly heterogeneous, being denser in the rostral than in the caudal MiA (Figs. 7a, 8a). Regarding to the MOB, in two injections (cases M1257 and M1209), the Mi presented very scarce labelling, with lightly stained somata observed in the lateral and medial aspects of the MOB (Table 2).

In the secondary olfactory centres, including the DTT, Pir and endopiriform nucleus, the distribution of retrograde labelling was similar to that observed after the injections in the MePV (Fig. 7b–h), although a lesser amount of retrogradely labelled cells was observed (Table 2).

Retrograde labelling in the amygdala and BST

In the vomeronasal amygdala, the injections in the MePD resulted only in a moderate amount of retrogradely labelled cells in the PMCo. This contrasts with the result obtained after MeA and MePV injections, in which the PMCo presented very dense labelling. The intranuclear distribution of the retrograde labelling follows the same pattern described following the injections in the MeA and MePV, that is, dense in its rostral and caudal parts (Fig. 7g, i, 8c), and moderate at intermediate levels (Fig. 7h).

Within the mixed chemosensory nuclei with vomeronasal predominance (Table 2), the MeA showed very dense labelling, with labelled cells located mainly at the caudal MeA (Fig. 7f). Noteworthy, in contrast to the results obtained following the injections in the MeA, at rostral levels the MeAD and MeAV subnuclei showed only moderate and very scarce labelling, respectively (Fig. 7e). More caudally, the MePV presented very dense labelling (Fig. 7g). The BAOT presented dense labelling (Fig. 7e), with darkly stained cells. Finally, the AAV and AAD showed very few labelled cells, in contrast with the moderate labelling observed after MeA and MePV injections (Table 2).

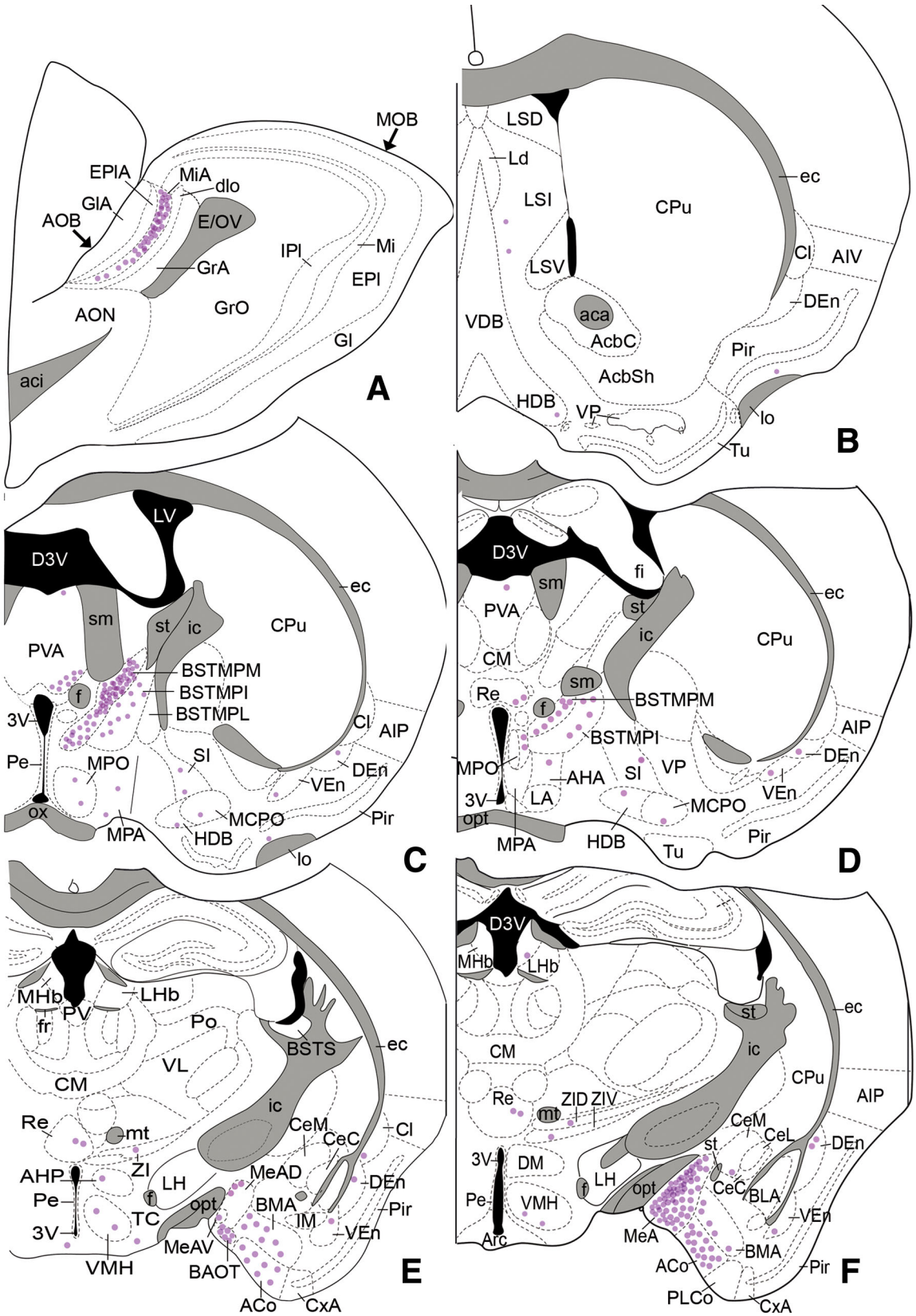
MOB
EPIA
MiA
dlo
GlA
AOB
E/OV
IPl
Mi
GrA
EPl
AON
GrO
Gl
aci
A
LSD
Ld
ec
LSl
CPu
LSV
Cl
AIV
DEn
VDB
aca
AcbC
Pir
AcbSh
HDB
VP
lo
Tu
B
LV
D3V
ec
sm
st
ic
CPu
PVA
BSTMPM
BSTMPI
BSTMPL
f
3V
Cl
AIP
Pe
MPO
SI
DEn
VEn
ox
MCPO
Pir
MPA
HDB
lo
C
D3V
fi
sm
ec
PVA
st
ic
CPu
CM
Re
sm
BSTMPM
f
BSTMPI
AIP
MPO
AHA
SI
VP
DEn
3V
LA
MCPO
VEn
opt
MPA
HDB
Tu
Pir
D
MHb
LHb
PV
fr
Po
BSTS
ec
VL
CM
ic
Re
mt
CeM
CeC
Cl
AHP
ZI
LH
MeAD
DEn
Pe
f
opt
BMA
IM
Pir
TC
3V
VEn
MeAV
VMH
BAOT
ACo
CxA
E
D3V
MHb
LHb
st
ec
CM
ic
CPu
AIP
Re
ZID
ZIV
mt
CeM
CeL
DEn
st
3V
DM
f
LH
opt
CeC
BLA
Pe
VMH
VEn
Arc
MeA
BMA
ACo
Pir
PLCo
CxA
F

◀**Fig. 7** Semi-schematic drawings of parasagittal (**a**) and frontal (**b**–**j**) sections through the mouse brain showing the distribution of retrogradely labelled somata following a fluorogold injection in the posterodorsal medial amygdaloid nucleus. The injection site is depicted in panel (**g**). **a** Is rostral, **j** is caudal. The semi-schematic drawings are based on case M1257, which presented the largest restricted injection. For abbreviations, see list

The structures composing the olfactory amygdala, including the mixed nuclei with olfactory predominance, showed less density of labelling following the injections in the MePD than after the injections in the MeA and MePV (Table 2). The densest labelling was observed in the ACo, mainly present in the caudal aspect of the nucleus (Fig. 7e, f). The PLCo presented moderate labelling, with darkly stained cells located mainly in the medial part of the layer II (Figs. 7g, h, 8b). In addition, the APir (Fig. 7i) and the LOT presented only a few labelled cells. Noteworthy, the CxA was devoid of labelled somata, in sharp contrast to what we observed in the case of MeA and MePV injections (Table 2; Fig. 7e, f).

Compared with the MeA and MePV injections, the basolateral complex was almost devoid of labelled cells with the exception of the BMA, which showed a moderate density a labelling (Fig. 7e, f). In addition, within the deep amygdaloid nuclei, the AHi presented, in general, a denser labelling than that observed following injections in the MeA and MePV, with retrogradely labelled cells located mainly in its rostral and medial aspect (Figs. 7g, h, 8c). Finally, within the central amygdala the CeM showed a low number of retrogradely labelled cells (as observed after injections in the MeA and MePD, Table 2), while the I and IM presented very scarce labelling (Fig. 7e–g).

Within the BST complex, unlike the MeA and MePV injections, only the BSTMPM, the BSTMPI and the BSTIA presented retrograde labelling (Table 2). The BSTMPM presented very dense labelling (much denser than after injections in the MeA and MePV, Table 2), with more labelled neurones present in its dorsal part (Figs. 4c, f, 7c). In contrast, the BSTMPI presented moderate labelling

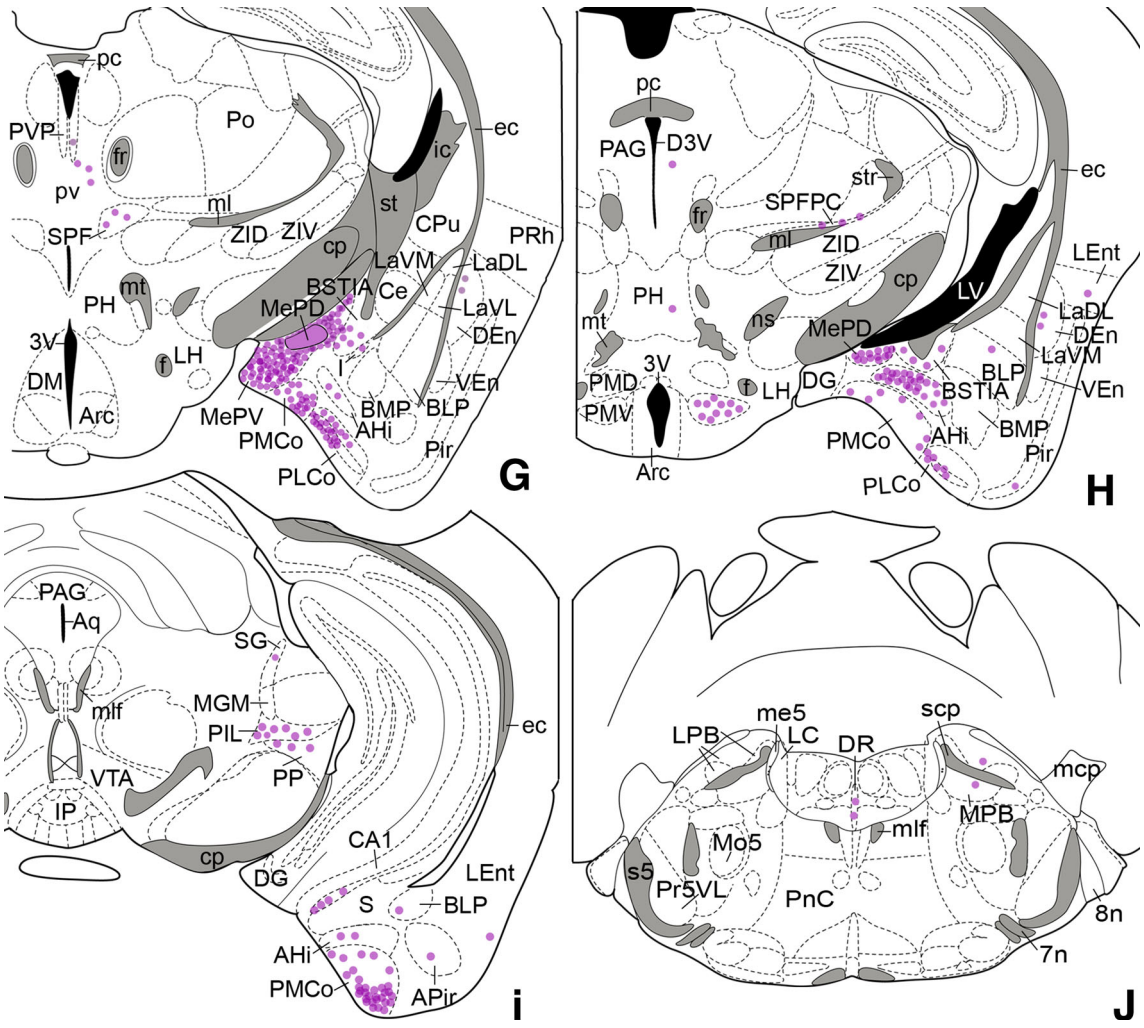

Fig. 7 continued

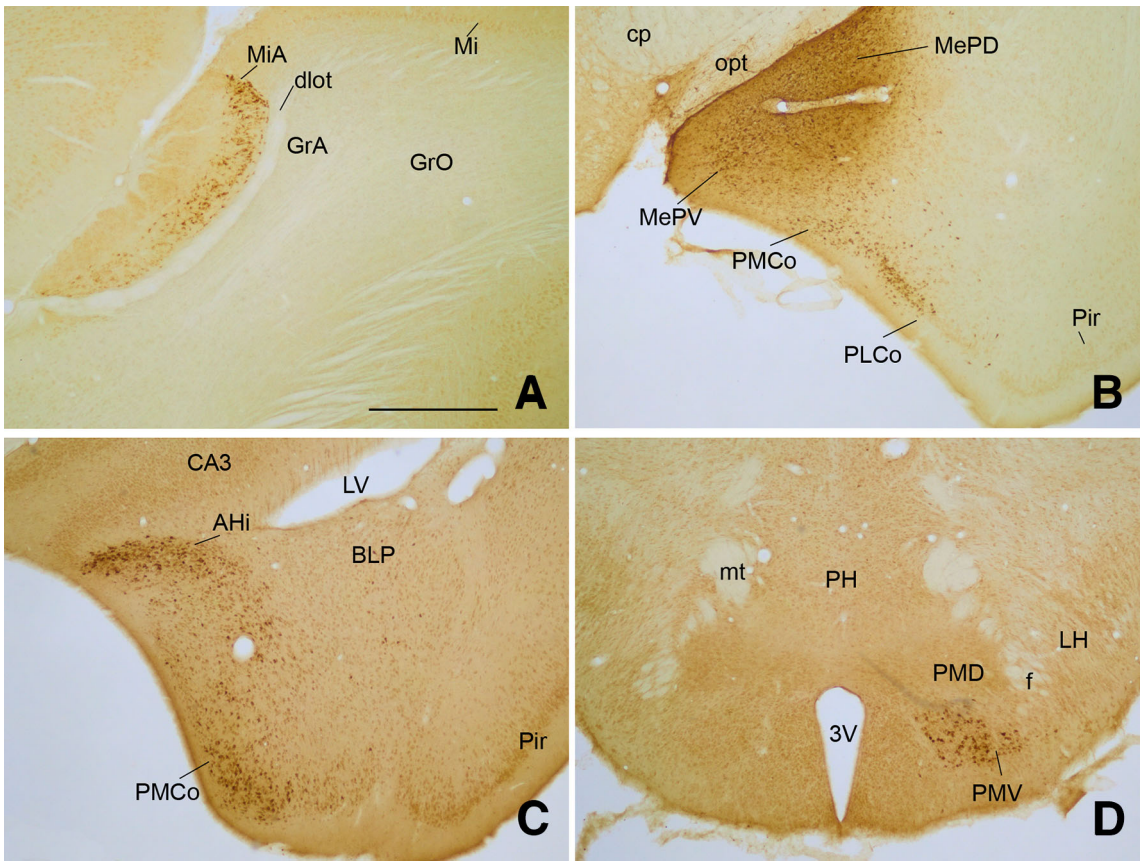

Fig. 8 Photomicrographs of parasagittal (**a**) and frontal (**b**–**d**) sections through the mouse forebrain, illustrating the retrograde labelling present in animals receiving a fluorogold injection in the posterodorsal medial amygdaloid nucleus (*MePD*). The images correspond to the retrograde labelling presented in the cases M1257 (**a**, **b**) and M1302 (**c**, **d**). **a** Retrogradely labelled mitral cells in the accessory olfactory bulb, mainly present in its anterior part. **b** Numerous labelled cells in the posteroventral medial amygdaloid subnucleus, as well as in the posterolateral cortical amygdaloid nucleus. Note that only scarce labelling is present at this level in the posteromedial cortical amygdaloid nucleus. **c** Dense retrograde labelling in the lateral aspect of the posteromedial cortical amygdaloid nucleus and in the medial part of the amygdalo-hippocampal area. **d** Retrogradely labelled cells in the ventral premammillary nucleus of the hypothalamus. For abbreviations, see list. *Scale bar* in **a** (valid for **b**–**d**): 500 μm

(Fig. 7c, d), less dense than following MeA or MePV injections. Finally, the BSTIA showed a moderate number of retrogradely labelled cells (Fig. 7g, h), similar to that observed after the MePV injections.

Retrograde labelling in the cerebral cortex, including the hippocampal formation

The retrograde labelling in mesocortical structures was very scarce following the injections in the MePD (and scarcer if compared with the results of injections in the MeA and MePD), with a few cells present in the MO, IL, DP, Cl and PRh (Table 2). Within the hippocampal formation, similar to the findings after injections in the MeA and MePV, the CA1 showed moderate labelling, with the labelled cells restricted to its ventral part (Fig. 7i), and a low number of labelled cells were observed in the LEnt (Fig. 7i).

Labelling in the septum and ventral forebrain

The distribution of the labelled somata within these areas was similar to that observed in the MeA and MePD injections. In the lateral septum, the LSI showed scarce labelling, and only a few labelled cells appeared in the LSV and SHi (Fig. 7b; Table 2). The MS and HDB/MCPO showed scarce labelling while the VDB presented very scarce labelling (Fig. 7b–d). Within the striato-pallidum, the SL and SI displayed scarce labelling.

Retrograde labelling in the thalamus

The injections in the MePD gave rise to a smaller number of retrogradely labelled cells in the anterior midline thalamus, but the location and distribution of labelled cells follow a similar pattern to that described following the injections in the MeA and MePV (Table 2; Figs. 4c, 7c–g).

In the posterior intralaminar thalamic complex, the distribution and density of the observed labelling was very similar to that described following the MeA and MePD injections (Fig. 7g–i), with the exception of the PP and SG which presented less labelled cells (Table 2).

Retrograde labelling in the hypothalamus

Retrograde labelling in the hypothalamus following the MePD injections differed from the one observed after the tracer injections in the MeA and MePD mainly in the PMV, the MPO and the VMH (Table 2). Within the preoptic hypothalamus, the MPO showed moderate labelling (only scarce labelling was obtained after the injections in the MeA and MePV), with darkly stained cells mainly located next to the BSTMPM (Fig. 7c, d; Table 2). Within the tuberal hypothalamus, the VMH presented scarce labelling (Fig. 7e, f), compared to the moderate labelling showed after the MeA and MePV injections (Table 2). Within the mammillary hypothalamus, the PMV showed very dense labelling (Figs. 7h, 8d), compared with the few labelled cells found after the MeA injections. Finally, in the anterior hypothalamus, and the rest of structures of the tuberal and mammillary hypothalamus, the observed labelling was very similar to that described after the injection in the MeA and MePV (Table 2).

Retrograde labelling in the midbrain and brainstem

The retrograde labelling obtained was virtually identical to that observed following the injections in the MePV (Fig. 7h–j; Table 2), with the PB being the only exception. It showed scarce labelling present both in its medial and lateral divisions (Fig. 7j).

Contralateral labelling

As described before in the MeA and MePV injections, the retrograde labelling found after FG injections in the MePD was mainly ipsilateral, and only a few labelled neurones were present in the contralateral hemisphere. Within the contralateral amygdala, the PMCo and MePV presented scarce labelling with darkly stained somata, and a few labelled cells were also present in the MeA and PLCo. In the BST, the BSTMPM and BSTMPI presented very scarce labelling. Within the septum and ventral forebrain, the MS, HBD and SL showed a very low number of labelled cells. Regarding to the thalamus, the SPF displayed scarce labelling, while the PVA, Re, SPFPC, PP and PIL presented only occasional labelling. Finally, within the hypothalamus, brainstem and midbrain the Arc, VMH, LH, TC, PMV, PH, PAG and PB showed a few scattered labelled cells.

Discussion

The results presented in this work describe for the first time, using restricted injections of retrograde tracers, the pattern of afferent projections to the main subdivisions of the Me in female mice. The results obtained confirm the general pattern of afferents to the Me (as a whole) inferred from a number of anterograde tracing studies in other rodents, mainly male rats and hamsters (see Pitkanen, 2000). This indicates that, despite the interspecies and intersexual differences in socio-sexual behaviours in which the Me is likely to be involved, the connectivity of the Me is similar. In addition, the analysis of the centripetal connections to the three subnuclei the medial amygdala reveals that, although a small number of differences in the inputs to the anterior, posteroventral and posterodorsal subdivisions of the Me exists, a common pattern of inputs predominates (see Fig. 9). The MePD is the subnucleus that shows more important differences in connectivity compared to the MeA and MePV, with these two subnuclei being more similar (see discussion below). The projections to all three medial amygdaloid subnuclei are mainly ipsilateral, although some of the afferent inputs are bilateral with ipsilateral predominance.

Projections to the medial amygdaloid nucleus from the olfactory system

Our results confirm and extend previous works that demonstrated that the Me receives convergent projections arising from the AOB and the MOB (Pro-Sistiaga et al. 2007; Kang et al. 2009; Cadiz-Moretti et al. 2013). The AOB provides massive inputs to the three subnuclei of the Me. These projections are a direct source of pheromonal information to the Me (Zufall and Leinders-Zufall 2007). In addition, our results reveal that the MePD is dominated by inputs from the anterior AOB, whereas the remaining divisions of the Me receive afferents from both AOB divisions (Fig. 9). Similar results have been reported in rats (Mohedano-Moriano et al. 2007). In addition, the work of Mohedano-Moriano et al. (2007) has also shown that the AOB projections to the BSTMPM originate in the rostral part of the AOB. The preferential projection from the anterior AOB to the MePD was not found in previous tracing studies in mice (retrograde: Salazar and Brennan 2001; anterograde: von Campenhausen and Mori 2000). However, Salazar and Brennan (2001) injected retrograde tracers only in the MeA and MePV, and therefore could not observe the differential retrograde labelling in the AOB. In the case of the injections of anterograde tracers in the rostral and caudal AOB divisions, it is difficult to detect a difference in the density of the anterograde labelling. However, a careful examination of the terminal fields in the

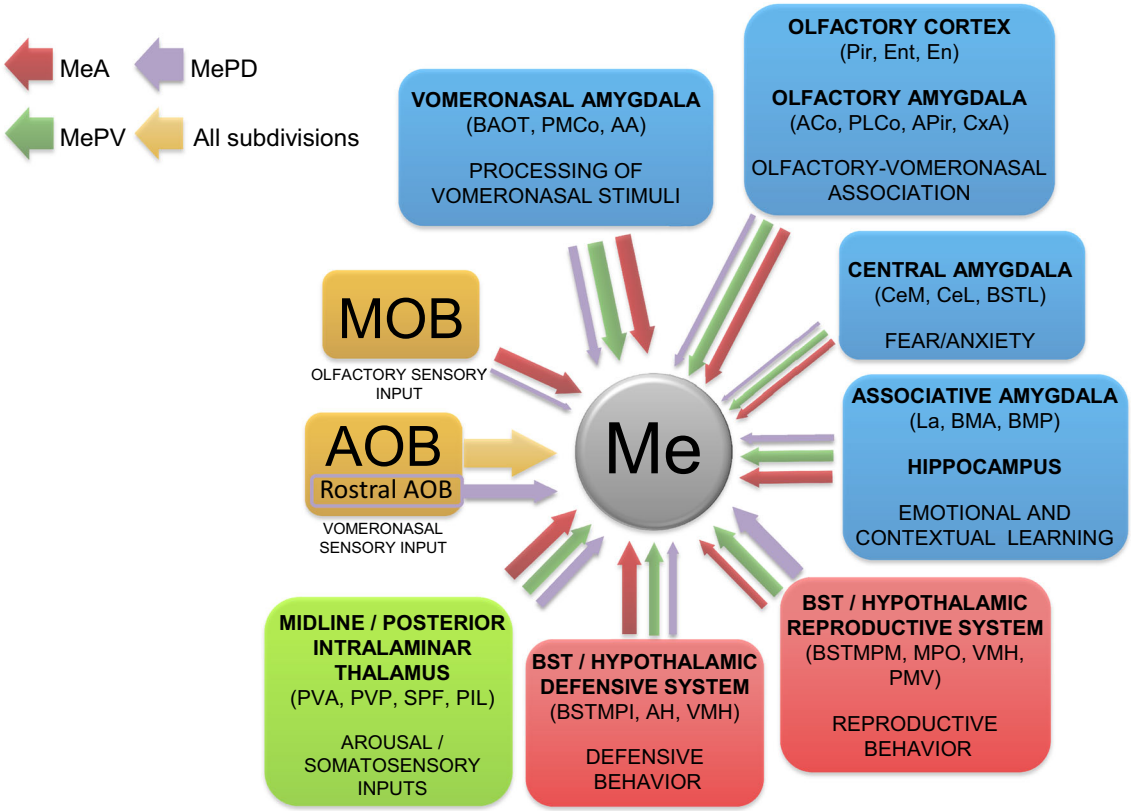

Fig. 9 Schematic diagram summarizing the main afferent projections to the medial amygdaloid nucleus, with indication of the relative density of the projections to its three subdivisions. The differential afferent projections to the different subdivisions are represented in *red* (*MeA*), *green* (*MePV*) and *violet* (*MePD*) colours. The *thickness* of the *arrows* roughly represents the density of the projections

MePD shown in the Fig. 4 of von Campenhausen and Mori (2000) suggests that the injections in the rostral AOB gave rise to a denser anterograde labelling in the MePD layer I.

Therefore, the anterior part of the AOB projects more strongly to the MePD and the BSTMPM, two structures strongly interconnected (present results, Pardo-Bellver et al. 2012). The rostral part of the AOB receives inputs from vomeronasal sensory neurones expressing the V1 type of receptors (V1R), which are activated by small, volatile molecules with pheromonal activity (Leinders-Zufall et al. 2000; Fortes-Marco et al. 2013). In contrast, the posterior AOB receives inputs from vomeronasal sensory neurones expressing the V2 type of receptors, which are activated by nonvolatile proteinaceous compounds of high molecular weight (Krieger et al. 1999; Fortes-Marco et al. 2013). Volatiles detected by V1R induce neuroendocrine effects (oestrous induction, puberty acceleration or delay, among others; see Halpern and Martinez-Marcos 2003) and therefore the MePD and BSTMPM may be particularly involved in mediating the effects of these volatile pheromones.

Regarding to the MOB, our results of retrograde tracing confirm that it sends moderate projections to the MeA and very weak projections to the MePD (Kang et al. 2009; Cadiz-Moretti et al. 2013; Fig. 9). As indicated in the results, of the three restricted injections in the MeA only one case was superficial enough as to encompass the terminal field of the MOB axons, which terminate even more superficial than the AOB projection (see Kang et al. 2009). In this case the retrograde labelling in the MOB was relatively dense. Another non-restricted injection affecting the superficial MeA and part of the SI located rostral to the MeA confirms this result. The scarcity of retrograde labelling observed in Figs. 2a and 3a is due to the deep location (the cell layer of the MeA) of the injection site in this case.

Among the structures receiving direct projections from both the AOB and MOB, the strongest degree of convergence is found in the MeA. Thus, on anatomical grounds, the MeA is the most important place of integration of vomeronasal and olfactory information within the amygdaloid complex (Petrulis 2013). In this regard, an unanswered question is the nature of the olfactory information relayed to the Me. An interesting possibility is that only mitral cells receiving information from sensory neurones with specialist receptors, such as those expressing TRPM5

(Thompson et al. 2012) innervate the Me. By this pathway, information about semiochemicals detected by the MOB may be integrated in the Me with the vomeronasal information relayed by the AOB. In agreement with this view, it has been shown that mitral cells of the MOB projecting to the Me are activated by male urinary volatiles in female mice, but not by female urinary volatiles or by predator odours (Kang et al. 2009). Moreover, olfactory sensory cells expressing a particular receptor, OR37C, innervate mitral cells that project specifically to the MePD (Bader et al. 2012). The sensory cells expressing receptors of the OR37 family respond to the presence of long-chain fatty aldehydes (Bautze et al. 2012), some of which are present in anal gland secretions (Bautze et al. 2014). These data reinforce the idea that the Me receives an olfactory input carrying information about specific semiochemicals.

Within the olfactory system, the olfactory cortex sends more projections to the MeA compared to the MePV, while it sends only very light projections to the MePD, in agreement with McDonald (1998). Regarding to the input from the Pir, the Me received stronger projections arising from the posterior Pir compared to the anterior Pir, corroborating previous descriptions (Christensen and Frederickson 1998).

Haberly (2001) suggested that the Pir functions more as an associative cortex than a primary sensory region. The posterior Pir presents more bidirectional connections with the amygdala than the anterior Pir (Haberly 2001). In addition, electrophysiological data revealed that, while the anterior Pir processes sensory information of the odorants, the posterior Pir shows associative encoding characteristics (Calu et al. 2007). Thus, the posterior Pir may act as an associative cortex that sends, mainly to the MeA and to a less extent to the MePV, highly processed olfactory information that includes the behavioural significance of the odorant.

Intramygdaloid projections to the medial amygdaloid nucleus

In agreement with our previous anterograde study (Pardo-Bellver et al. 2012), the injections of retrograde tracers in the different Me subnuclei confirmed the existence of a dense and intricate set of intranuclear connections. Previous anatomical and functional data obtained in hamsters (Meredith and Westberry 2004; Maras and Petrulis 2010a, b, c) and mice (Choi et al. 2005; Samuelsen and Meredith 2009a, b) have suggested that the MeA would act as a filter for the chemosensory information received from the bulbs. From the MeA, conspecific-related information would be sent through the MePD and predator-related information through the MePV. Our results show that the interconnections between the MePD and MePV allow the activity in each one of these subnuclei to influence the other. In addition, both the MePV and the MePD project back to the MeA (as shown previously in rats, Canteras et al. 1995), and therefore the information flow through the Me is, by no means, unidirectional.

The Me shows also an important set of intraamygdaloid inputs, originated mainly in other nuclei of the chemosensory amygdala (Gutiérrez-Castellanos et al. 2010; Fig. 9). As shown by previous anterograde (rat: Canteras et al. 1995; mice: Gutiérrez-Castellanos et al. 2014), and retrograde (hamster: Coolen and Wood 1998) tracing studies, the PMCo gives rise to an important projection to all three Me subnuclei, allowing strong intraamygdaloid processing of vomeronasal information. The Me is composed to a large extent by neurones originated in subpallial territories (Bupesh et al. 2011), whereas the PMCo is a cortical structure (Gutiérrez-Castellanos et al. 2014). The projection from the PMCo to the Me can therefore be interpreted as a cortico-subcortical pathway within the vomeronasal system. This view is supported by retrograde tracing experiments with sodium selenide, revealing that the projection from the PMCo to the Me is originated by zinc-positive (putative glutamatergic) cells (Christensen and Frederickson 1998). Like in other circuits of the cerebral hemispheres, the cortical component, the PMCo, is mainly involved in intratelencephalic pathways (Gutiérrez-Castellanos et al. 2014), while the subcortical element (the Me) gives rise to the major extratelencephalic outputs (Canteras et al. 1995; Pardo-Bellver et al. 2012). Our results also indicate that the projection from the PMCo to the MePD is apparently less dense than to the other Me subnuclei (thus confirming previous anterograde tracing data, Gutiérrez-Castellanos et al. 2014) and arises preferentially from a specific portion of this nucleus, suggesting the possibility of a topographical organization of this cortico-subcortical pathway within the vomeronasal system. This possibility, however, needs experimental confirmation.

The Me also receives projections from the amygdalar BAOT and AA, which receive a predominant input from the AOB. In the latter case, however, it is noteworthy that the projection from the AA innervates mainly the anterior and posteroventral Me subnuclei. Although there is little information available on the connections and function of the AA (Martínez-García et al. 2012), this finding suggests that it is more related to the MeA and MePV than to the MePD, which in turn is the Me subnucleus more strongly involved in reproductive-related functions (Simerly 2002).

In contrast with the strong inputs to the Me originated in the vomeronasal amygdala, the olfactory amygdaloid nuclei are heterogeneous regarding their projections to the Me. The PLCo and CoA give rise to important projections to the Me, whereas the CxA, APir and LOT originate only a light projection to the Me. The inputs from the CxA, APir

and LOT target mainly the MeA and MePV, as exemplified by the projection from the APir (see Table 2). Therefore, on anatomical grounds, the MePD is less influenced by the olfactory information processed in the amygdaloid nuclei. Similar results regarding the projections from the olfactory amygdala to the Me were observed in rats and hamsters (Coolen and Wood 1998; Pitkanen, 2000; Majak and Pitkanen 2003).

The deep structures of the amygdala, namely the basolateral complex and the central nucleus, originate only minor projections to the Me, with the exception of the basomedial nucleus, which has an important interconnections with the MeA (present results; Petrovich et al. 1996; Pardo-Bellver et al. 2012). The MePV receives also a moderate projection from the basomedial nucleus, whereas the MePD shows only very minor afferents from the basolateral amygdaloid complex. In contrast, the MePD receives an important projection from the AHi, in agreement with previous anterograde data (Canteras et al. 1992a). This is consistent with the interpretation that the AHi is strongly related to the vomeronasal system (see Swanson and Petrovich 1998; Martínez-García et al. 2012). Regarding the central amygdala, its medial subdivision gives rise to a very light projection to the Me. These afferents are reciprocated by a much denser projection from the Me to the medial Ce (Pardo-Bellver et al. 2012). We hypothesize that this connection may play a role in the fear behaviour elicited by predator-derived chemicals. In fact, recent findings show that the Me is critically involved in the acquisition (and expression) of olfactory conditioned fear (Cousens et al. 2012). In addition, lesions of the basolateral complex (encompassing the lateral nucleus and neighbouring structures) also abolish olfactory fear conditioning (Cahill and McGaugh 1990; Cousens and Otto 1998). Since both the Me and the basolateral complex play a key role in olfactory fear conditioning, the direct interconnections between the Me and the basomedial nucleus (present results, Canteras et al. 1995; Petrovich et al. 1996; Pardo-Bellver et al. 2012) may provide the link allowing the information related to the odour-shock association to be integrated in both structures.

Afferent projections to the medial amygdaloid nucleus from the bed nucleus of the stria terminalis

The interconnections of the BST with the Me and the central amygdala constitute the canonical circuit of the so-called extended amygdala. The concept of extended amygdala stems in the observations that the amygdala seems to extend into the basal telencephalon (see de Olmos et al. 2004), where portions of the BST, the sublenticular substantia innominata and the interstitial nucleus of the posterior limb of the anterior commissure, show similar neurochemical and hodological properties to the Me and Ce. This allows recognising two divisions in the extended amygdala. The medial extended amygdala is interconnected with the Me with which it shares some hodological and neurochemical properties, whereas the central extended amygdala is reciprocally connected with the Ce and has connections and neurochemical markers similar to it (see Olucha-Bordonau et al. 2015).

In line with this, the BSTMP, the main structure of the medial extended amygdala, is one of the main targets of the efferent projections of the Me (Gomez and Newman 1992; Canteras et al. 1995; Coolen and Wood 1998; Dong et al. 2001; Pardo-Bellver et al. 2012). The present experiments show that, by contrast, the projections from the BST back to the Me are, on anatomical grounds, not so important (although this not necessarily means lack of functional relevance). Exceptions to this rule are the afferents from the posteromedial subdivisions of the BST (BSTMPI and BSTMPM), which, together with the BSTIA, give rise to substantial projections to the Me subnuclei. These projections are topographically organized: the BSTMPI projects preferentially to the MeA and MePV, whereas the BSTMPM innervates preferentially the MePD (Fig. 9). The reciprocal projection between the BSTMPM and the MePD reinforces the view that these nuclei are part of the network of sexually dimorphic nuclei (Guillamon and Segovia 1997; Gu et al. 2003) enriched in receptors for sexual steroids (Simerly et al. 1990; Mitra et al. 2003) that control socio-sexual behaviours (Newman 1999; Swann et al. 2009). The reciprocal projection between the BSTMPI and the MeA is consistent with the mixed projections of both structures to the defensive and reproductive behavioural control columns of the hypothalamus (Canteras et al. 1995; Pardo-Bellver et al. 2012; Swanson 2000). The MePV, as in other cases, is similar in this respect to the MeA. The compartment-specific interconnections between the Me and posteromedial subdivisions of the BST suggest the existence of two subsystems within the medial extended amygdala. On the one hand, the MePD-BSTMPM is strongly dominated by a vomeronasal input (reaching both nuclei) mainly arising from V1R-expressing sensory neurones (see above: "Projections to the Me from the olfactory system"). This subsystem of the medial extended amygdala shows a clear sexual dimorphism attaining the size and cell number (Morris et al. 2008; Tsukahara et al. 2011). On the other hand, the MeA is interconnected mainly with the BSTMPI, where sexual dimorphism is less apparent, but affects at least a population of vasopressinergic cells (Rood et al. 2013; Otero-Garcia et al. 2014). This subsystem received mixed olfactory and vomeronasal inputs (reaching only the MeA). Finally, the MePV shows intermediate features, as it is interconnected with both BSTMPM and BSTMPI.

Afferent projections to the medial amygdaloid nucleus from cortical areas including the hippocampus

According to our results, only allocortical and mesocortical areas project to the Me. Within the mesocortex, the AI shows consistently, moderate density of retrograde labelling after injections to the MeA. In association with this labelling, a few labelled cells are usually found in the claustrum, a pallial derivative that occupies a location deep to the insula. The projection from the insula has been previously shown with anterograde tracing experiments in rats (McDonald et al. 1996; McDonald 1998; Shi and Cassell 1998). The projections from the AI to the MeA may be involved in the relay of multimodal sensory information (McDonald 1998; Shi and Cassell 1998). The projection to the Me also originates in the posterior AI, which probably relays somatosensory information that may play a role in the relay of footshock information (unconditioned stimulus) in fear conditioning paradigms (Shi and Davis 1999).

The prefrontal cortex also sends projections to the Me, to a larger degree to the MeA than to the MePV and MePD, which apparently receive very light prefrontal inputs. The main prefrontal afferent to the Me arises from the IL (present results in mice; Hurley et al. 1991; McDonald et al. 1996; McDonald 1998, in rats). The IL projection to the amygdala is involved in the extinction of fear conditioning (Sierra-Mercado et al. 2011), and therefore the projection of the IL to the Me may play a similar role in the case of olfactory fear conditioning, which depends on the Me (Cousens et al. 2012).

Within the allocortex, the hippocampal formation (sensu lato) shows important projections to the Me, with differences among its subnuclei. Thus, our results indicate that the retrograde labelling in the caudal CA1, ventral subiculum and LEnt is abundant after injections into the MeA, less abundant when injections were centred in the MePV and even less after tracer injections in the MePD. Previous works described a similar pattern of projections in the rat, using both retrograde (Christensen and Frederickson 1998) and anterograde tracer experiments (Canteras and Swanson 1992; McDonald 1998; Kishi et al. 2006; Cenquizca and Swanson 2007). These projections are reciprocal, since the Me also projects to the ventral CA1, subiculum and LEnt (Canteras et al. 1995; Pardo-Bellver et al. 2012). Although there are no functional data indicating a possible role of the ventral CA1 projections to the Me, it seems that the ventral hippocampus is specifically involved in defense/fear-related behaviour (Kjelstrup et al. 2002), probably in relation with the processing of the contextual stimuli (Maren and Fanselow 1995; Zhang et al. 2001). This subregion of the ventral CA1 is also connected with the PMCo (Gutiérrez-Castellanos et al. 2014) and projects to the AOB (de la Rosa-Prieto et al. 2009). We hypothesize that the anatomical interconnections described between the vomeronasal system and the ventral hippocampus allow pheromonal and spatial information to be integrated, and consequently modulate the behavioural response to chemicals signals as a function of the spatial context (e.g., own versus alien territory).

Afferent projections to the medial amygdala from the basal telencephalon

Within the septum and striatum, the medial septum, diagonal band/MCPO, SL and SI presented the most important inputs to the Me (showing a moderate to scarce projection).

Previous works have described that the MCPO (Nitecka 1981) and HDB (Ottersen 1980) send projections to the Me, although these works did not differentiated between the subdivisions of the Me. Our results confirm and extend these findings. Similar to the inputs described for the cortex, the MeA receives the strongest projection, the MePD the weakest, and the MePV is intermediate between those two.

The MS, diagonal band and MCPO are classified as the medial group of the septal region (Risold 2004). This region has important connections with the ventral (temporal) hippocampal field, entorhinal and prefrontal cortex (Risold 2004), areas that send, as described in the present work, projections to the Me (predominantly to the MeA). The MS may have a role in maintaining the arousal level required for sexual activity (Gulia et al. 2008), and possible also other Me-related behaviours consequently its input to the Me may influence the activity of this nucleus in this context.

Projections to the medial amygdaloid nucleus from the hypothalamus

Our results show that the Me receives relatively minor projections arising from hypothalamic nuclei, with four exceptions: the PMV, VMH, PH and MPO. The PMV sends massive projections to the MePV and MePD. The VMH and PH send moderate projections to the MeA and MePV, and finally the MPO sends moderate projections to the MePD.

Within the entire hypothalamus, only the PMV projects massively to the Me. This nucleus shows strong projections to the MePD and MePV, while it presents only light projections to the MeA. The important projection arising from the PMV to the MePD is consistent with previous works in male rats (Ottersen 1980; Canteras et al. 1992b). Canteras et al. (1992b) described also a moderate projection to the rostral part of the MeA, which we observed as scarce in our preparations, probably as a result of the small size of our injections. In contrast to our results, Canteras et al. (1992b)

found no projection from the PMV to the MePV in male rats. Possible explanations of this discrepancy may be either interspecific differences or sexual dimorphism, since we used female mice our experiments. Further studies are needed to clarify these inconsistencies.

The PMV displays strong bidirectional connections with the MePD and MePV (present findings, Canteras et al. 1995; Pardo-Bellver et al. 2012), and with sexually dimorphic areas related to reproductive and aggressive behaviours, as well as to neuroendocrine zones of the hypothalamus (Canteras et al. 1992b). It is part of a hypothalamic circuit involved in the control of reproductive behaviour (Swanson 2000), and in fact it is strongly influenced by gonadal steroid hormones (Canteras et al. 1992b). The PMV shows high levels of c-fos expression in male mice exposed to female soiled bedding (Yokosuka et al. 1999), but also in female rats during maternal aggression experiments (Motta et al. 2013). Furthermore, in male hamsters it is activated by both mating and agonistic interactions (Kollack-Walker and Newman 1995). Therefore, as suggested by Yokosuka et al. (1999), this nucleus may play an important role in the control of the motivation of copulatory and/or aggressive behaviour. Thus, the PMV, by means of its massive feedback input to the MePV and MePD may be modulating the chemosensory processing in these subdivisions of the Me, probably in relation with the behavioural response (reproductive or aggressive) that the animal is executing.

Regarding the afferents from the preoptic hypothalamus, consistent with our results a projection from the MPO to the Me was described previously in rats (Ottersen 1980). We extend this finding showing that the MPO projects mainly to the MePD, and to a lesser extent also to the MeA and MePV. Since the MPO is part of the reproductive-related hypothalamic circuit (Swanson 2000), this finding further supports the hypothesis that the MePD is more related with sexual behaviour.

The VMH and PH send moderate projections to the MeA and MePV and scarce projections to the MePD. Previous works have reported that the VMH projects more densely to the rostral part of the MeA compared to the other Me subnuclei, and described that these projections to the Me originate mainly from the central and the dorsomedial parts of the VMH (Ottersen 1980; Canteras et al. 1994). Our results in female mice partially contrast with these data in male rats, since we found that the MeA and MePV receive more projections from the VMH than the MePD, and found no differences in the origin of these projections according to the VMH subdivisions. The ventrolateral division of the VMH has been proposed to be part of the reproductive behavioural control column of the hypothalamus, whereas its dorsomedial division would be part of the defensive circuit (Swanson 2000; Choi et al. 2005). However, recent electrophysiological data and optogenetic activation experiments have revealed that within the ventrolateral VMH there are neuronal populations involved in mating and conspecific aggression (Lin et al. 2011; Falkner et al. 2014). Therefore, without further characterization of the properties of the retrogradely labelled cells in the VMH, it is not possible to known whether the feedback projection they provide to the Me is related to sexual or aggressive behaviours.

Previous works have reported projections arising from the PH to the medial amygdala (Nitecka 1981; Vertes et al. 1995), which in turn projects (although lightly) to the PH (Pardo-Bellver et al. 2012). The PH projects to a number of subcortical and cortical "limbic-related" structures, and it has been suggested to be involved in various components of emotional behaviour, including emotional learning (Vertes et al. 1995). In this regard, it integrates cardiorespiratory and motor responses and controls the theta rhythm of the hippocampus (Vertes et al. 1995).

Finally, with regard to the minor hypothalamic afferents to the Me, previous works in the rat have reported, consistent with our results, light projections arising from the AH (Risold et al. 1994), DM (Thompson et al. 1996), Arc (Ottersen 1980; Krieger et al. 1979) and LH (Nitecka 1981; Ottersen 1980; Veening 1978) to the Me. A minor discrepancy with the present results is the presence of a moderate projection from the TC to the Me (Nitecka 1981; Canteras et al. 1994), which we observed to be scarce.

Projections from the thalamus and brainstem to the medial nucleus of the amygdala

The thalamic afferents to the Me arise mainly from the midline and posterior intralaminar nuclei. These afferents are common to the three Me subnuclei, although the projection to the MePD tends to be somewhat lighter than that of the MeA and MePV (Table 2; Fig. 9). The midline thalamic nuclei that project to the Me are the paraventricular and reuniens, both of which also receive projections from the Me (Canteras et al. 1995; Pardo-Bellver et al. 2012). The afferent projection from the paraventricular thalamic nucleus to the Me has been previously described in rats (Li and Kirouac 2008; Vertes and Hoover 2008). This thalamic nucleus is related to arousal and attention processes, and therefore its input to the Me may modulate the attention towards the chemical signals processed in the Me.

The afferent projections from the posterior intralaminar thalamic complex (encompassing the SG, MGM, PIN, SPF, PIL and PP) to the Me are very similar to those described from the same structures to the central and lateral nuclei of the amygdala (Turner and Herkenham 1991). These projections have been shown to relay auditory (LeDoux et al.

1990a), somatosensory (LeDoux et al. 1987; Bordi and LeDoux 1994; Lanuza et al. 2008) and visual (Doron and LeDoux 1999; Linke et al. 1999) information, and play a key role in the acquisition of fear conditioning (LeDoux et al. 1990b). It is not known whether the same neurones of the posterior intralaminar thalamic complex project to both the Me and the central and lateral amygdaloid nuclei. In any case, it is likely that this thalamic projection sends (at least) somatosensory information to the Me, given that it is necessary in the acquisition of olfactory fear conditioning (Cousens et al. 2012) and shows increased expression of c-Fos following the delivery of footshock (Pezzone et al. 1992; Rosen et al. 1998).

A very different kind of somatosensory information that has been shown to activate the medial amygdala is that derived from vaginocervical stimulation (Erskine 1993; Pfaus et al. 1993, 1996; Polston and Erskine 1995; Tetel et al. 1993). The somatosensory genital information may reach the Me through the thalamic SPF (Veening and Coolen 1998). The convergence of genital somatosensory information with chemosensory information (about odorants and pheromones) would take place in the Me, thus allowing the association of chemical cues with the reinforcing mating experience. This kind of olfactory-genitosensory learning in the Me may be the reason that explains why sexually experienced animals with lesions of the vomeronasal organ show very small deficits in sexual behaviour (Meredith 1986).

Finally, within the brainstem the main afferent projection to the Me is originated by the parabrachial nucleus. This nucleus may relay visceroceptive (from its medial aspect) and nociceptive information (from its lateral aspect) (Fulwiler and Saper 1984; Bourgeais et al. 2001; Lanuza et al. 2004). We found retrogradely labelled neurones both in the medial and lateral parabrachial nucleus, mainly following tracer injections in the MeA. These afferents may relay sensory information relevant to associate chemical stimuli with aversive learning (such as olfactory fear conditioning).

Connections of the medial amygdala subnuclei and their role in defensive and socio-sexual behaviours

The results of the present study show that the three subdivisions of the Me receive a similar pattern of afferent projections, with some quantitative differences in the density of the neural inputs from particular structures and a few qualitative differences. For instance, the MePD shows very reduced inputs from the mesocortex (prefrontal and insular areas).

Previous works studying the efferent projections of the Me have emphasized these differences, and functional data relate the MePD with reproductive-related behaviours and the MePV with defensive behaviours. Although our findings do not contradict this view, for both the afferents (present results) and the efferents (Canteras et al. 1995; Pardo-Bellver et al. 2012), we observe connections between the MePD and hypothalamic nuclei related with defensive behaviour, such as the anterior hypothalamic area and the dorsomedial VMH. In the same vein, non-negligible connections are present between the MePV and the hypothalamic reproductive-related nuclei, such as the MPO, the ventrolateral part of the VMH and the PMV. Therefore, on anatomical grounds, the segregation between these two systems is not clear. Instead, the differences between the connectivity of the MePD and MePV are mainly a matter of relative density, with basically the same pattern of connections shared by both subnuclei (Fig. 9). Regarding the anterior part of the Me, it is very similar to the MePV, i.e., it shows relevant connections with hypothalamic nuclei related to reproductive and defensive behaviours. In conclusion, although differential afferents and efferents of the Me subnuclei with the hypothalamic networks for socio-sexual (MePD) and defensive responses (MePV) might suggest differential roles in these behaviours, this is not as clear as it may seem. First, differences in these connections are not qualitative (clear-cut) but just quantitative. Second, the three subnuclei of the Me show very important reciprocal connections (see results). And third, all three subnuclei are deeply interconnected with the BST (with some differences), and the complex Me-BST-hypothalamic interconnections (Dong and Swanson 2004; Dong et al. 2001) may blur the effects of activation of a single subnucleus of the Me on behaviour.

This view is also supported by data on c-fos expression. Thus, male mice exposed to female urine show an increase c-Fos expression in all subdivisions of the Me (Samuelsen and Meredith 2009a, b), not just the MePD, and similar results were obtained in female mice exposed to male-soiled bedding (Halem et al. 1999; Moncho-Bogani et al. 2005). In addition, odours from heterospecifics (including predators and non-predators) were observed to induce c-Fos expression in the MeA (Meredith and Westberry 2004; Samuelsen and Meredith 2009a, b). A specific c-fos induction in the MePV was found in rats (Dielenberg et al. 2001) and mice (Choi et al. 2005) exposed to cat odours, although, as detailed above, the MePV also respond to conspecifics of the same and opposite sex (Meredith and Westberry 2004; Samuelsen and Meredith 2009a, b). A recent multisite extracellular recording study in mice in the MePD and MePV found that, although neurones responding to conspecific stimuli were more often located dorsally in the posterior Me, and neurones responding to predator urinary stimuli were more often located ventrally, there were also individual cells distributed throughout the posterior Me responding to conspecific and defensive stimuli

(Bergan et al. 2014). In summary, the chemical cues described to activate the MeA and MePV (in addition to sexually related odours and odours from same sex conspecifics), include odours from ill conspecifics (Arakawa et al. 2010), and from predators (Takahashi 2014). Consistent with these functional data, the MeA and MePV have been suggested to play a general role in the categorization of the chemical cues detected (mainly) by the vomeronasal organ and acting as a filter to convey appropriate chemosensory information to the MePD or other downstream targets (Meredith and Westberry 2004; Samuelsen and Meredith 2009a, b; Maras and Petrulis 2010a, b, c). In contrast, the MePD, according to both anatomical and functional data, has been proposed to be specifically involved in the control of sexual behaviour (Swann et al. 2009). However, in rats the MePD is also activated following aggressive encounters between males (Veening et al. 2005), and thus it may play a role also in agonistic interactions. Finally, we want to note that the Me (as a whole) is involved in olfactory fear conditioning, as well as in learning to fear the context where the predator odours were presented (Takahashi et al. 2007).

In summary, the Me is involved in the unconditioned responses elicited by social and sexual cues, as well as predator-derived chemicals, and also in learning to associate olfactory cues with aversive (and maybe appetitive) experiences. However, our anatomical data suggest that the subdivisions of the Me play cooperative rather than differential roles in the control of socio-sexual vs antipredatory behaviours.

Acknowledgments Funded by the Spanish Ministry of Science-FEDER (BFU2010-16656 and BFU2013-47688-P). B.C.-M. is a predoctoral fellow of the "Becas Chile" program of the Government of Chile.

References

Arakawa H, Arakawa K, Deak T (2010) Oxytocin and vasopressin in the medial amygdala differentially modulate approach and avoidance behavior toward illness-related social odor. Neuroscience 171:1141–1151

Bader A, Breer H, Strotmann J (2012) Untypical connectivity from olfactory sensory neurons expressing OR37 into higher brain centers visualized by genetic tracing. Histochem Cell Biol 137:615–628

Bautze V, Bar R, Fissler B, Trapp M, Schmidt D, Beifuss U, Bufe B, Zufall F, Breer H, Strotmann J (2012) Mammalian-specific OR37 receptors are differentially activated by distinct odorous fatty aldehydes. Chem Senses 37:479–493

Bautze V, Schwack W, Breer H, Strotmann J (2014) Identification of a natural source for the OR37B ligand. Chem Senses 39:27–38

Bergan JF, Ben-Shaul Y, Dulac C (2014) Sex-specific processing of social cues in the medial amygdala. Elife 3:e02743. doi:10.7554/eLife02743

Bordi F, LeDoux JE (1994) Response properties of single units in areas of rat auditory thalamus that project to the amygdala. II. Cells receiving convergent auditory and somatosensory inputs and cells antidromically activated by amygdala stimulation. Exp Brain Res 98:275–286

Bourgeais L, Gauriau C, Bernard JF (2001) Projections from the nociceptive area of the central nucleus of the amygdala to the forebrain: a PHA-L study in the rat. Eur J Neurosci 14:229–255

Bupesh M, Legaz I, Abellan A, Medina L (2011) Multiple telencephalic and extratelencephalic embryonic domains contribute neurons to the medial extended amygdala. J Comp Neurol 519:1505–1525

Cadiz-Moretti B, Martinez-Garcia F, Lanuza E (2013) Neural substrate to associate odorants and pheromones: convergence of projections from the main and accessory olfactory bulbs in mice. In: East ML, Dehnhard M (eds) Chemical signals in vertebrates 12. Springer Science, New York, pp 3–16

Cahill L, McGaugh JL (1990) Amygdaloid complex lesions differentially affect retention of tasks using appetitive and aversive reinforcement. Behav Neurosci 104:532–543

Calu DJ, Roesch MR, Stalnaker TA, Schoenbaum G (2007) Associative encoding in posterior piriform cortex during odor discrimination and reversal learning. Cereb Cortex 17:1342–1349

Canteras NS, Swanson LW (1992) Projections of the ventral subiculum to the amygdala, septum, and hypothalamus: a PHAL anterograde tract-tracing study in the rat. J Comp Neurol 324:180–194

Canteras NS, Simerly RB, Swanson LW (1992a) Connections of the posterior nucleus of the amygdala. J Comp Neurol 324:143–179

Canteras NS, Simerly RB, Swanson LW (1992b) Projections of the ventral premammillary nucleus. J Comp Neurol 324:195–212

Canteras NS, Simerly RB, Swanson LW (1994) Organization of projections from the ventromedial nucleus of the hypothalamus: a *Phaseolus vulgaris*-leucoagglutinin study in the rat. J Comp Neurol 348:41–79

Canteras NS, Simerly RB, Swanson LW (1995) Organization of projections from the medial nucleus of the amygdala: a PHAL study in the rat. J Comp Neurol 360:213–245

Cenquizca LA, Swanson LW (2007) Spatial organization of direct hippocampal field CA1 axonal projections to the rest of the cerebral cortex. Brain Res Rev 56:1–26

Chamero P, Marton TF, Logan DW, Flanagan K, Cruz JR, Saghatelian A, Cravatt BF, Stowers L (2007) Identification of protein pheromones that promote aggressive behaviour. Nature 450:899–902

Choi GB, Dong HW, Murphy AJ, Valenzuela DM, Yancopoulos GD, Swanson LW, Anderson DJ (2005) Lhx6 delineates a pathway mediating innate reproductive behaviors from the amygdala to the hypothalamus. Neuron 46:647–660

Christensen MK, Frederickson CJ (1998) Zinc-containing afferent projections to the rat corticomedial amygdaloid complex: a retrograde tracing study. J Comp Neurol 400:375–390

Coolen LM, Wood RI (1998) Bidirectional connections of the medial amygdaloid nucleus in the Syrian hamster brain: simultaneous anterograde and retrograde tract tracing. J Comp Neurol 399:189–209

Cousens G, Otto T (1998) Both pre- and posttraining excitotoxic lesions of the basolateral amygdala abolish the expression of olfactory and contextual fear conditioning. Behav Neurosci 112:1092–1103

Cousens GA, Kearns A, Laterza F, Tundidor J (2012) Excitotoxic lesions of the medial amygdala attenuate olfactory fear-potentiated startle and conditioned freezing behavior. Behav Brain Res 229:427–432

de la Rosa-Prieto C, Ubeda-Banon I, Mohedano-Moriano A, Pro-Sistiaga P, Saiz-Sanchez D, Insausti R, Martinez-Marcos A (2009) Subicular and CA1 hippocampal projections to the accessory olfactory bulb. Hippocampus 19:124–129

de Olmos JS, Beltramino CA, Alheid GF (2004) Amygdala and extended Amygdala of the rat: a cytoarchitectonical, fibroarchitectonical, and chemoarchitectonical survey. In: Paxinos G (ed) The rat nervous system. Elsevier Academic Press, San Diego, pp 509–603

Dielenberg RA, Hunt GE, McGregor IS (2001) "When a rat smells a cat": the distribution of Fos immunoreactivity in rat brain following exposure to a predatory odor. Neuroscience 104:1085–1097

Dong HW, Swanson LW (2004) Projections from bed nuclei of the stria terminalis, posterior division: implications for cerebral hemisphere regulation of defensive and reproductive behaviors. J Comp Neurol 471:396–433

Dong HW, Petrovich GD, Swanson LW (2001) Topography of projections from amygdala to bed nuclei of the stria terminalis. Brain Res Rev 38:192–246

Doron NN, LeDoux JE (1999) Organization of projections to the lateral amygdala from auditory and visual areas of the thalamus in the rat. J Comp Neurol 412:383–409

Erskine MS (1993) Mating-induced increases in FOS protein in preoptic area and medial amygdala of cycling female rats. Brain Res Bull 32:447–451

Falkner AL, Dollar P, Perona P, Anderson DJ, Lin D (2014) Decoding ventromedial hypothalamic neural activity during male mouse aggression. J Neurosci 34:5971–5984

Fortes-Marco L, Lanuza E, Martinez-Garcia F (2013) Of pheromones and kairomones: what receptors mediate innate emotional responses? Anat Rec (Hoboken) 296:1346–1363

Fulwiler CE, Saper CB (1984) Subnuclear organization of the efferent connections of the parabrachial nucleus in the rat. Brain Res 319:229–259

Gomez DM, Newman SW (1992) Differential projections of the anterior and posterior regions of the medial amygdaloid nucleus in the Syrian hamster. J Comp Neurol 317:195–218

Goodson JL (2005) The vertebrate social behavior network: evolutionary themes and variations. Horm Behav 48:11–22

Gu G, Cornea A, Simerly RB (2003) Sexual differentiation of projections from the principal nucleus of the bed nuclei of the stria terminalis. J Comp Neurol 460:542–562

Guillamon A, Segovia S (1997) Sex differences in the vomeronasal system. Brain Res Bull 44:377–382

Gulia KK, Jodo E, Kawauchi A, Miki T, Kayama Y, Mallick HN, Koyama Y (2008) The septal area, site for the central regulation of penile erection during waking and rapid eye movement sleep in rats: a stimulation study. Neuroscience 156:1064–1073

Gutiérrez-Castellanos N, Martínez-Marcos A, Martínez-García F, Lanuza E (2010) Chemosensory function of the amygdala. Vitam Horm 83:165–196

Gutiérrez-Castellanos N, Pardo-Bellver C, Martínez-García F, Lanuza E (2014) The vomeronasal cortex—afferent and efferent projections of the posteromedial cortical nucleus of the amygdala in mice. Eur J Neurosci 39:141–158

Haberly LB (2001) Parallel-distributed processing in olfactory cortex: new insights from morphological and physiological analysis of neuronal circuitry. Chem Senses 26:551–576

Halem HA, Cherry JA, Baum MJ (1999) Vomeronasal neuroepithelium and forebrain Fos responses to male pheromones in male and female mice. J Neurobiol 39:249–263

Halpern M, Martinez-Marcos A (2003) Structure and function of the vomeronasal system: an update. Prog Neurobiol 70:245–318

Hari Dass SA, Vyas A (2014) Copulation or sensory cues from the female augment fos expression in arginine vasopressin neurons of the posterodorsal medial amygdala of male rats. Front Zool 11:42

Hurley KM, Herbert H, Moga MM, Saper CB (1991) Efferent projections of the infralimbic cortex of the rat. J Comp Neurol 308:249–276

Isogai Y, Si S, Pont-Lezica L, Tan T, Kapoor V, Murthy VN, Dulac C (2011) Molecular organization of vomeronasal chemoreception. Nature 478:241–245

Kang N, Baum MJ, Cherry JA (2009) A direct main olfactory bulb projection to the 'vomeronasal' amygdala in female mice selectively responds to volatile pheromones from males. Eur J Neurosci 29:624–634

Kang N, Baum MJ, Cherry JA (2011) Different profiles of main and accessory olfactory bulb mitral/tufted cell projections revealed in mice using an anterograde tracer and a whole-mount, flattened cortex preparation. Chem Senses 36:251–260

Kishi T, Tsumori T, Yokota S, Yasui Y (2006) Topographical projection from the hippocampal formation to the amygdala: a combined anterograde and retrograde tracing study in the rat. J Comp Neurol 496:349–368

Kjelstrup KG, Tuvnes FA, Steffenach HA, Murison R, Moser EI, Moser MB (2002) Reduced fear expression after lesions of the ventral hippocampus. Proc Natl Acad Sci USA 99:10825–10830

Kollack-Walker S, Newman SW (1995) Mating and agonistic behavior produce different patterns of fos immunolabeling in the male Syrian hamster brain. Neurosci 66:721–736

Koolhaas JM, van den Brink THC, Roozendaal B, Boorsma F (1990) Medial amygdala and aggressive behavior: interaction between testosterone and vasopressin. Aggr Behav 16:223–229

Krieger MS, Conrad LC, Pfaff DW (1979) An autoradiographic study of the efferent connections of the ventromedial nucleus of the hypothalamus. J Comp Neurol 183:785–815

Krieger J, Schmitt A, Lobel D, Gudermann T, Schultz G, Breer H, Boekhoff I (1999) Selective activation of G protein subtypes in the vomeronasal organ upon stimulation with urine-derived compounds. J Biol Chem 274:4655–4662

Lanuza E, Nader K, LeDoux JE (2004) Unconditioned stimulus pathways to the amygdala: effects of posterior thalamic and cortical lesions on fear conditioning. Neuroscience 125:305–315

Lanuza E, Moncho-Bogani J, LeDoux JE (2008) Unconditioned stimulus pathways to the amygdala: effects of lesions of the posterior intralaminar thalamus on foot-shock-induced c-Fos expression in the subdivisions of the lateral amygdala. Neuroscience 155:959–968

LeDoux JE, Ruggiero DA, Forest R, Stornetta R, Reis DJ (1987) Topographic organization of convergent projections to the thalamus from the inferior colliculus and spinal cord in the rat. J Comp Neurol 264:123–146

LeDoux JE, Farb C, Ruggiero DA (1990a) Topographic organization of neurons in the acoustic thalamus that project to the amygdala. J Neurosci 10:1043–1054

LeDoux JE, Cicchetti P, Xagoraris A, Romanski LM (1990b) The lateral amygdaloid nucleus: sensory interface of the amygdala in fear conditioning. J Neurosci 10:1062–1069

Lehman MN, Winans SS, Powers JB (1980) Medial nucleus of the amygdala mediates chemosensory control of male hamster sexual behavior. Science 210:557–560

Leinders-Zufall T, Lane AP, Puche AC, Ma W, Novotny MV, Shipley MT, Zufall F (2000) Ultrasensitive pheromone detection by mammalian vomeronasal neurons. Nature 405:792–796

Li S, Kirouac GJ (2008) Projections from the paraventricular nucleus of the thalamus to the forebrain, with special emphasis on the extended amygdala. J Comp Neurol 506:263–287

Lin D, Boyle MP, Dollar P, Lee H, Lein ES, Perona P, Anderson DJ (2011) Functional identification of an aggression locus in the mouse hypothalamus. Nature 470:221–226

Linke R, De Lima AD, Schwegler H, Pape HC (1999) Direct synaptic connections of axons from superior colliculus with identified thalamo-amygdaloid projection neurons in the rat: possible substrates of a subcortical visual pathway to the amygdala. J Comp Neurol 403:158–170

Majak K, Pitkanen A (2003) Projections from the periamygdaloid cortex to the amygdaloid complex, the hippocampal formation, and the parahippocampal region: a PHA-L study in the rat. Hippocampus 13:922–942

Maras PM, Petrulis A (2010a) Anatomical connections between the anterior and posterodorsal sub-regions of the medial amygdala: integration of odor and hormone signals. Neuroscience 170:610–622

Maras PM, Petrulis A (2010b) The anterior medial amygdala transmits sexual odor information to the posterior medial amygdala and related forebrain nuclei. Eur J Neurosci 32:469–482

Maras PM, Petrulis A (2010c) Lesions that functionally disconnect the anterior and posterodorsal sub-regions of the medial amygdala eliminate opposite-sex odor preference in male Syrian hamsters (*Mesocricetus auratus*). Neuroscience 165:1052–1062

Maren S, Fanselow MS (1995) Synaptic plasticity in the basolateral amygdala induced by hippocampal formation stimulation in vivo. J Neurosci 15:7548–7564

Martínez-García F, Novejarque A, Gutiérrez-Castellanos N, Lanuza E (2012) Piriform cortex and amygdala. In: Watson C, Paxinos G, Puelles L (eds) The mouse nervous system. Academic Press, San Diego, pp 140–172

McDonald AJ (1998) Cortical pathways to the mammalian amygdala. Prog Neurobiol 55:257–332

McDonald AJ, Mascagni F, Guo L (1996) Projections of the medial and lateral prefrontal cortices to the amygdala: a *Phaseolus vulgaris* leucoagglutinin study in the rat. Neuroscience 71:55–75

Meredith M (1986) Vomeronasal organ removal before sexual experience impairs male hamster mating behavior. Physiol Behav 36:737–743

Meredith M, Westberry JM (2004) Distinctive responses in the medial amygdala to same-species and different-species pheromones. J Neurosci 24:5719–5725

Mitra SW, Hoskin E, Yudkovitz J, Pear L, Wilkinson HA, Hayashi S, Pfaff DW, Ogawa S, Rohrer SP, Schaeffer JM, McEwen BS, Alves SE (2003) Immunolocalization of estrogen receptor beta in the mouse brain: comparison with estrogen receptor alpha. Endocrinology 144:2055–2067

Mohedano-Moriano A, Pro-Sistiaga P, Ubeda-Banon I, Crespo C, Insausti R, Martinez-Marcos A (2007) Segregated pathways to the vomeronasal amygdala: differential projections from the anterior and posterior divisions of the accessory olfactory bulb. Eur J Neurosci 25:2065–2080

Moncho-Bogani J, Martinez-Garcia F, Novejarque A, Lanuza E (2005) Attraction to sexual pheromones and associated odorants in female mice involves activation of the reward system and basolateral amygdala. Eur J Neurosci 21:2186–2198

Morgan HD, Watchus JA, Milgram NW, Fleming AS (1999) The long lasting effects of electrical simulation of the medial preoptic area and medial amygdala on maternal behavior in female rats. Behav Brain Res 99:61–73

Morris JA, Jordan CL, King ZA, Northcutt KV, Breedlove SM (2008) Sexual dimorphism and steroid responsiveness of the posterodorsal medial amygdala in adult mice. Brain Res 1190:115–121

Motta SC, Guimaraes CC, Furigo IC, Sukikara MH, Baldo MV, Lonstein JS, Canteras NS (2013) Ventral premammillary nucleus as a critical sensory relay to the maternal aggression network. Proc Natl Acad Sci USA 110:14438–14443

Newman SW (1999) The medial extended amygdala in male reproductive behavior. A node in the mammalian social behavior network. Ann N Y Acad Sci 877:242–257

Nitecka L (1981) Connections of the hypothalamus and preoptic area with nuclei of the amygdaloid body in the rat; HRP retrograde transport study. Acta Neurobiol Exp 41:53–67

Nodari F, Hsu FF, Fu X, Holekamp TF, Kao LF, Turk J, Holy TE (2008) Sulfated steroids as natural ligands of mouse pheromone-sensing neurons. J Neurosci 28:6407–6418

Olucha-Bordonau FE, Fortes-Marco L, Otero-García M, Lanuza E, Martínez-García F (2015) Amygdala, structure and function. In: Paxinos G (ed) The rat nervous system. Academic Press, New York, pp 441–490

Otero-Garcia M, Martin-Sanchez A, Fortes-Marco L, Martínez-Ricós J, Agustin-Pavón C, Lanuza E, Martínez-García F (2014) Extending the socio-sexual brain: arginine-vasopressin immunoreactive circuits in the telencephalon of mice. Brain Struct Funct 219:1055–1081

Ottersen OP (1980) Afferent connections of the amygdaloid complex of the rat and cat. II. Afferents from the hypothalamus and the basal telencephalon. J Comp Neurol 194:267–289

Ottersen OP, Ben-Ari Y (1979) Afferent connections of the amygdaloid complex of the rat and cat. I. Projections from the thalamus. J Comp Neurol 187:401–424

Oxley G, Fleming AS (2000) The effects of medial preoptic area and amygdala lesions on maternal behavior in the juvenile rat. Dev Psychobiol 37:253–265

Palomero-Gallagher N, Zilles K (2015) Isocortex. In: Paxinos G (ed) The rat nervous system, 4th edn. Academic Press, London, pp 601–625

Papes F, Logan DW, Stowers L (2010) The vomeronasal organ mediates interspecies defensive behaviors through detection of protein pheromone homologs. Cell 141:692–703

Pardo-Bellver C, Cadiz-Moretti B, Novejarque A, Martinez-Garcia F, Lanuza E (2012) Differential efferent projections of the anterior, posteroventral, and posterodorsal subdivisions of the medial amygdala in mice. Front Neuroanat 6:33

Paxinos G, Franklin KBJ (2001) The mouse brain in stereotaxic coordinates. Academic Press, San Diego

Petrovich GD, Risold PY, Swanson LW (1996) Organization of projections from the basomedial nucleus of the amygdala: a PHAL study in the rat. J Comp Neurol 374:387–420

Petrulis A (2013) Chemosignals, hormones and mammalian reproduction. Horm Behav 63:723–741

Pezzone MA, Lee W-, Hoffman GE, Rabin BS (1992) Induction of c-Fos immunoreactivity in the rat forebrain by conditioned and unconditioned aversive stimuli. Brain Res 597:41–50

Pfaus JG, Kleopoulos SP, Mobbs CV, Gibbs RB, Pfaff DW (1993) Sexual stimulation activates c-fos within estrogen-concentrating regions of the female rat forebrain. Brain Res 624:253–267

Pfaus JG, Marcangione C, Smith WJ, Manitt C, Abillamaa H (1996) Differential induction of Fos in the female rat brain following different amounts of vaginocervical stimulation: modulation by steroid hormones. Brain Res 741:314–330

Pitkanen A (2000) Connectivity of the rat amygdaloid complex. In: Aggleton J (ed) The amygdala. A functional analysis, 2nd edn. Oxford University Press, Oxford, pp 31–115

Polston EK, Erskine MS (1995) Patterns of induction of the immediate-early genes c-fos and egr-1 in the female rat brain following differential amounts of mating stimulation. Neuroendocrinology 62:370–384

Pro-Sistiaga P, Mohedano-Moriano A, Ubeda-Banon I, Del Mar Arroyo-Jimenez M, Marcos P, Artacho-Perula E, Crespo C, Insausti R, Martinez-Marcos A (2007) Convergence of olfactory and vomeronasal projections in the rat basal telencephalon. J Comp Neurol 504:346–362

Puelles L, Kuwana E, Puelles E, Bulfone A, Shimamura K, Keleher J, Smiga S, Rubenstein JL (2000) Pallial and subpallial derivatives in the embryonic chick and mouse telencephalon, traced by the expression of the genes dlx-2, emx-1, nkx- 2.1, pax-6, and tbr-1. J Comp Neurol 424:409–438

Risold PY (2004) The septal region. In: Paxinos G (ed) The rat nervous system, 3rd edn. Academic Press, San Diego, pp 605–632

Risold PY, Canteras NS, Swanson LW (1994) Organization of projections from the anterior hypothalamic nucleus: a *Phaseolus vulgaris*-leucoagglutinin study in the rat. J Comp Neurol 348:1–40

Riviere S, Challet L, Fluegge D, Spehr M, Rodriguez I (2009) Formyl peptide receptor-like proteins are a novel family of vomeronasal chemosensors. Nature 459:574–577

Rood BD, Stott RT, You S, Smith CJ, Woodbury ME, De Vries GJ (2013) Site of origin of and sex differences in the vasopressin innervation of the mouse (*Mus musculus*) brain. J Comp Neurol 521:2321–2358

Rosen JB, Fanselow MS, Young SL, Sitcoske M, Maren S (1998) Immediate-early gene expression in the amygdala following footshock stress and contextual fear conditioning. Brain Res 796:132–142

Salazar I, Brennan PA (2001) Retrograde labelling of mitral/tufted cells in the mouse accessory olfactory bulb following local injections of the lipophilic tracer DiI into the vomeronasal amygdala. Brain Res 896:198–203

Samuelsen CL, Meredith M (2009a) Categorization of biologically relevant chemical signals in the medial amygdala. Brain Res 1263:33–42

Samuelsen CL, Meredith M (2009b) The vomeronasal organ is required for the male mouse medial amygdala response to chemical-communication signals, as assessed by immediate early gene expression. Neuroscience 164:1468–1476

Sano K, Tsuda MC, Musatov S, Sakamoto T, Ogawa S (2013) Differential effects of site-specific knockdown of estrogen receptor alpha in the medial amygdala, medial pre-optic area, and ventromedial nucleus of the hypothalamus on sexual and aggressive behavior of male mice. Eur J Neurosci 37:1308–1319

Scalia F, Winans SS (1975) The differential projections of the olfactory bulb and accessory olfactory bulb in mammals. J Comp Neurol 161:31–55

Shi CJ, Cassell MD (1998) Cortical, thalamic, and amygdaloid connections of the anterior and posterior insular cortices. J Comp Neurol 399:440–468

Shi C, Davis M (1999) Pain pathways involved in fear conditioning measured with fear-potentiated startle: lesion studies. J Neurosci 19:420–430

Sierra-Mercado D, Padilla-Coreano N, Quirk GJ (2011) Dissociable roles of prelimbic and infralimbic cortices, ventral hippocampus, and basolateral amygdala in the expression and extinction of conditioned fear. Neuropsychopharmacology 36:529–538

Simerly RB (2002) Wired for reproduction: organization and development of sexually dimorphic circuits in the mammalian forebrain. Annu Rev Neurosci 25:507–536

Simerly RB, Chang C, Muramatsu M, Swanson LW (1990) Distribution of androgen and estrogen receptor mRNA-containing cells in the rat brain: an in situ hybridization study. J Comp Neurol 294:76–95

Swann J, Fabre-Nys C, Barton R (2009) Hormonal and pheromonal modulation of the extended amygdala: implications for social behavior. In: Pfaff DW, Arnold AP, Fahrbach SE, Etgen AM, Rubin RT (eds) Hormones, brain and behavior, 2nd edn. Academic Press, San Diego, pp 441–474

Swanson LW (2000) Cerebral hemisphere regulation of motivated behavior. Brain Res 886:113–164

Swanson LW, Petrovich GD (1998) What is the amygdala? Trends Neurosci 21:323–331

Tachikawa KS, Yoshihara Y, Kuroda KO (2013) Behavioral transition from attack to parenting in male mice: a crucial role of the vomeronasal system. J Neurosci 33:5120–5126

Takahashi LK (2014) Olfactory systems and neural circuits that modulate predator odor fear. Front Behav Neurosci 8:72

Takahashi LK, Hubbard DT, Lee I, Dar Y, Sipes SM (2007) Predator odor-induced conditioned fear involves the basolateral and medial amygdala. Behav Neurosci 121:100–110

Tetel MJ, Getzinger MJ, Blaustein JD (1993) Fos expression in the rat brain following vaginal-cervical stimulation by mating and manual probing. J Neuroendocrinol 5:397–404

Thompson RH, Canteras NS, Swanson LW (1996) Organization of projections from the dorsomedial nucleus of the hypothalamus: a PHA-L study in the rat. J Comp Neurol 376:143–173

Thompson JA, Salcedo E, Restrepo D, Finger TE (2012) Second-order input to the medial amygdala from olfactory sensory neurons expressing the transduction channel TRPM5. J Comp Neurol 520:1819–1830

Tirindelli R, Dibattista M, Pifferi S, Menini A (2009) From pheromones to behavior. Physiol Rev 89:921–956

Tsukahara S, Tsuda MC, Kurihara R, Kato Y, Kuroda Y, Nakata M, Xiao K, Nagata K, Toda K, Ogawa S (2011) Effects of aromatase or estrogen receptor gene deletion on masculinization of the principal nucleus of the bed nucleus of the stria terminalis of mice. Neuroendocrinology 94(2):137–147

Turner BH, Herkenham M (1991) Thalamoamygdaloid projections in the rat: a test of the amygdala's role in sensory processing. J Comp Neurol 313:295–325

Usunoff KG, Schmitt O, Itzev DE, Haas SJ, Lazarov NE, Rolfs A, Wree A (2009) Efferent projections of the anterior and posterodorsal regions of the medial nucleus of the amygdala in the mouse. Cells Tissues Organs 190:256–285

Veening JG (1978) Subcortical afferents of the amygdaloid complex in the rat: an HRP study. Neurosci Lett 8:197–202

Veening JG, Coolen LM (1998) Neural activation following sexual behavior in the male and female rat brain. Behav Brain Res 92:181–193

Veening JG, Coolen LM, de Jong TR, Joosten HW, de Boer SF, Koolhaas JM, Olivier B (2005) Do similar neural systems subserve aggressive and sexual behaviour in male rats? Insights from c-Fos and pharmacological studies. Eur J Pharmacol 526:226–239

Vertes RP, Hoover WB (2008) Projections of the paraventricular and paratenial nuclei of the dorsal midline thalamus in the rat. J Comp Neurol 508:212–237

Vertes RP, Crane AM, Colom LV, Bland BH (1995) Ascending projections of the posterior nucleus of the hypothalamus: PHA-L analysis in the rat. J Comp Neurol 359:90–116

von Campenhausen H, Mori K (2000) Convergence of segregated pheromonal pathways from the accessory olfactory bulb to the cortex in the mouse. Eur J Neurosci 12:33–46

Wang Y, He Z, Zhao C, Li L (2013) Medial amygdala lesions modify aggressive behavior and immediate early gene expression in oxytocin and vasopressin neurons during intermale exposure. Behav Brain Res 245:42–49

Yokosuka M, Matsuoka M, Ohtani-Kaneko R, Iigo M, Hara M, Hirata K, Ichikawa M (1999) Female-soiled bedding induced fos immunoreactivity in the ventral part of the premammillary nucleus (PMv) of the male mouse. Physiol Behav 68:257–261

Zhang WN, Bast T, Feldon J (2001) The ventral hippocampus and fear conditioning in rats: different anterograde amnesias of fear after infusion of *N*-methyl-D-aspartate or its noncompetitive antagonist MK-801 into the ventral hippocampus. Behav Brain Res 126:159–174

Zufall F, Leinders-Zufall T (2007) Mammalian pheromone sensing. Curr Opin Neurobiol 17:483–489